People's Democratic Republic of Algeria
Ministry of Higher Education and Scientific Research

Kasdi Merbah University, Ouargla

Faculty of Hydrocarbons, Renewable Energies, Earth and Universe Sciences

Hydrocarbon production department

MEMORY:

To obtain the Master's degree

Option:

Production Academic

THEME

Asphaltene Characterization Using XRD and Field Flow Assurance Assessment: Zone 01 Samples and OMM-33 Crude Oil

Presented by:

Mr. BERREDJEM Mohamed Islem
Mr. BENNACEUR Hamza

Jury:

President: KADRI Ahmed Yacine.

Examiner: DJEBBAS Faycal.

Supervisor: DADA Saada.

Defended on: 06/15/2025 12:00 p.m.

2024/2025

Table of Contents:

Tables of Figures:

List of tables:

Gratitude:

*First of all, we thank our **Allah** the merciful and the merciful for having given us the strength and the patience to carry out this modest work.*

*We thank our **parents** for their support and encouragement during our studies.*

Finally, we would like to thank everyone who contributed directly or indirectly to the success of this work

Dedication:

I dedicate this modest work

To my dearest Mother and Father.

My dedication also goes to my dear brothers and sisters.

To all the teachers at Hydrocarbons, Especially the supervisor Dada Saada.

And we would to give a special thanks to Mr.Meryouma Abderraouf, Mr. Bensedik Mohamed, Mr Mahboub Youcef and all the engineer in the Sonatrach Irrara how helped us to make this work.

Hamza Bennaceur and Berredjem Mohamed Islem

Abstract:

This thesis investigated the properties of asphaltenes from Algeria's Hassi Messaoud oil field, focusing on their characterization and implications for flow assurance. X-ray Diffraction (XRD) analysis of extracted asphaltenes revealed a significant paraffinic character alongside their polyaromatic cores, with relatively loose aromatic sheet stacking (d002 ≈ 4.00-4.05 Å). A case study on crude oil from well OMM-33 confirmed a high Asphaltene Onset Pressure (AOP), significantly exceeding bubble point pressures and initial reservoir pressure, indicating a high precipitation risk even in single-phase liquid. Dynamic deposition tests showed substantial asphaltene-rich deposits at 90°C (97.7% asphaltene) and mixed organic deposits (44.4% asphaltene) at 75°C, highlighting temperature-dependent deposit composition. These findings suggest that Hassi Messaoud asphaltenes, with their notable paraffinic association and high precipitation tendency, pose complex flow assurance challenges that may not be adequately addressed by traditional mitigation strategies, underscoring the need for advanced, tailored solutions.
Key words: Asphaltene, precipitation, X-ray Diffraction (XRD), Asphaltene onset pressure, Deposition, PVT analysis.

Résumé:

Cette thèse a examiné les propriétés des asphaltènes du champ pétrolier de Hassi Messaoud en Algérie, en se concentrant sur leur caractérisation et leurs implications pour la garantie de l'écoulement. L'analyse par diffraction des rayons X (DRX) des asphaltènes extraits a révélé un caractère paraffinique significatif aux côtés de leurs noyaux polyaromatiques, avec un empilement relativement lâche des feuillets aromatiques (d002 ≈ 4,00-4,05 Å). Une étude de cas sur le pétrole brut du puits OMM-33 a confirmé une Pression de Début de Précipitation des Asphaltènes (PDPA) élevée, dépassant de manière significative les pressions de point de bulle et la pression initiale du réservoir, indiquant un risque élevé de précipitation même en phase liquide monophasique. Des tests de dépôt dynamique ont montré des dépôts substantiels riches en asphaltènes à 90°C (97,7 % d'asphaltènes) et des dépôts organiques mixtes (44,4 % d'asphaltènes) à 75°C, soulignant une composition de dépôt dépendante de la température. Ces résultats suggèrent que les asphaltènes de Hassi Messaoud, avec leur association paraffinique notable et leur forte tendance à la précipitation,

posent des défis complexes pour la garantie de l'écoulement qui pourraient ne pas être adéquatement résolus par les stratégies d'atténuation traditionnelles, soulignant le besoin de solutions avancées et personnalisées.

Mots clés : Asphaltène, précipitation, diffraction des rayons X (DRX), pression de formation d'asphaltène, dépôt, analyse PVT.

ملخص:

بحثت هذه الأطروحة في خصائص الأسفلتينات من حقل حاسي مسعود النفطي بالجزائر، مع التركيز على توصيفها وتأثيراتها على ضمان التدفق. كشف تحليل حيود الأشعة السينية (XRD) للأسفلتينات المستخلصة عن طابع برافيني بارز إلى جانب نواتها العطرية متعددة الحلقات، مع تراكب فضفاض نسبياً للصفائح العطرية 4.05-4.00 ≈ d002) .(Åوأكدت دراسة حالة على النفط الخام من بئر OMM-33 ارتفاع ضغط بدء ترسب الأسفلتينات(AOP) ، متجاوزاً بشكل كبير ضغوط نقطة الفقاعة والضغط الأولي للمكمن، مما يشير إلى خطر ترسب عالٍ حتى في الطور السائل أحادي المرحلة. أظهرت اختبارات الترسب الديناميكي وجود ترسبات كبيرة غنية بالأسفلتين عند 90 درجة مئوية (97.7% أسفلتين) وترسبات عضوية مختلطة (44.4% أسفلتين) عند 75 درجة مئوية، مما يسلط الضوء على تركيبة ترسب تعتمد على درجة الحرارة. تشير هذه النتائج إلى أن أسفلتينات حاسي مسعود، بارتباطها البرافيني الملحوظ وميلها العالي للترسب، تطرح تحديات معقدة لضمان التدفق قد لا تعالجها استراتيجيات التخفيف التقليدية بشكل كافٍ، مما يؤكد الحاجة إلى حلول متقدمة ومصممة خصيصاً.

الكلمات المفتاحية: الأسفلتين، الترسيب، حيود الأشعة السينية(XRD) ، ضغط بداية تكوين الأسفلتين، الترسيب، تحليل PVT.

Nomenclature:

Symbol / Term	Description	Unit / Notes
AOP	Asphaltene Onset Pressure – pressure at which asphaltenes begin to precipitate	psig
API	American Petroleum Institute gravity – measures oil density	°API
d_{002}	Interlayer spacing between stacked aromatic layers (from XRD)	Å (angstroms)
La	Average lateral size of aromatic clusters (from XRD, (10) band)	Å (angstroms)
β (FWHM)	Full Width at Half Maximum – peak broadening parameter in XRD	Radians or degrees
λ	Wavelength of X-ray radiation (Cu Kα commonly used = 1.54 Å)	Å
θ (Theta)	Diffraction angle in Bragg's law	Degrees
Bo	Formation volume factor of oil	m^3/stb or m^3/m^3
Bg	Formation volume factor of gas	m^3/stm^3
SARA	Saturates, Aromatics, Resins, Asphaltenes	–
H/C ratio	Hydrogen-to-carbon atomic ratio – indicates aromaticity	Dimensionless
FTIR	Fourier Transform Infrared Spectroscopy – identifies functional groups	–
FTIR A1600	FTIR absorption peak for aromatic C=C bonds	cm^{-1}
FTIR A140 / A2900	FTIR absorption peaks for aliphatic C–H bonds	cm^{-1}
I_{1600}/I_{2900}	FTIR-based aromaticity index	–

Nomenclature:

Symbol / Term	Description	Unit / Notes
XRD	X-ray Diffraction – identifies crystalline structure and ordering	–
NMR	Nuclear Magnetic Resonance – evaluates carbon structure	–
^{13}C NMR	Carbon-13 NMR – distinguishes aromatic vs aliphatic carbons	ppm
SEM	Scanning Electron Microscopy – surface morphology analysis	–
T	Temperature	°C
P	Pressure	bar or psig
V	Vanadium content (trace metal, usually in porphyrin form)	ppm
Ni	Nickel content (trace metal)	ppm
S	Sulfur content – heteroatom common in asphaltenes	wt%
N	Nitrogen content – heteroatom in heterocyclic structures	wt%
C	Carbon content	wt%
H	Hydrogen content	wt%
O	Oxygen content	wt% (often calculated)
ppm	Parts per million	–
wt%	Weight percent	%
Ra, R2, R3	Reservoir zones within the Cambro-Ordovician formation in HMD	–
HMD	Hassi Messoud field	–
ASTM	American Society for Testing and Materials	–

Nomenclature:

Symbol / Term	Description	Unit / Notes
ICP	Inductively Coupled Plasma	–
ICP-MS	ICP-Mass Spectrometry	–
ICP-OES	ICP-Optical Emission Spectroscopy	–
XRF	X-Ray Fluorescence	–
COSY	Correlation Spectroscopy	–
HSQC	Heteronuclear Single Quantum Coherence	–
HMBC	Heteronuclear Multiple Bond Correlation	–

Nomenclature:

Symbol / Term	Description
ASTM D287	Standard Test Method for API Gravity of Crude Petroleum and Petroleum Products (Hydrometer Method), Used to determine the API gravity using a hydrometer. This is a basic and widely used method in labs.
ASTM D1298	Standard Test Method for Density, Relative Density, or API Gravity of Crude Petroleum and Liquid Petroleum Products by Hydrometer Method Similar to D287 but includes more detailed steps for calculating density and API gravity using hydrometers at different temperatures.
ASTM D97	Standard Test Method for Pour Point of Petroleum Products. Used to Measures the lowest temperature at which a petroleum liquid can still flow. It helps assess cold flow behavior and wax/asphaltene solidification risk during storage, transport, or production.
ASTM D1217	Standard Test Method for Density and Relative Density (Specific Gravity) of Liquids by Bingham Pycnometer. Used to Measures the specific gravity of petroleum liquids using a pycnometer, giving high-precision results.

General Introduction:

Crude oil is a complex mixture of hydrocarbons and non-hydrocarbon compounds whose behavior during production and processing is strongly influenced by its composition. Among its most problematic components are asphaltenes—heavy, polar, and high-molecular-weight molecules that can precipitate under certain changes in pressure, temperature, or composition. Asphaltene precipitation and deposition are major contributors to flow assurance problems, leading to production losses, equipment blockage, and formation damage.

As part of the development of oil exploitation and refining techniques, it is important to accurately understand the structure and behavior of its various constituents. Indeed, crude oil is composed of four families (SARA): saturated hydrocarbons, aromatics, resins, and asphaltenes. This distribution is very broad; each part of crude oil also consists of a range of molecules with variable structures and properties, in the case of the Hassi Messaoud field (0.08 to 0.2%), particularly in Zone 1.

This research focuses on the physicochemical characterization of asphaltenes of Hassi Messaoud field specifically zone 1, using methods such as elemental analysis, XRD (X-ray diffraction). Real production data, including pressure–temperature profiles and deposition tests from well OMM-33, are also used to assess the risk of asphaltene precipitation during oil flow.

The aim of this work is:

Improve knowledge of asphaltenes by getting better understanding to the asphaltene conditions formation and their structure and behavior in order to develop more reliable prevention and mitigation strategies for oil production systems in Hassi Messaoud and similar reservoirs.

Chapter I: Introduction To Crude Oil and Asphaltene.

I.1. Introduction To Hassi Messaoud field:

The Hassi Messaoud field is located in the vast desert of the Algerian Sahara, north of the African continent. at 700km southeast of the capital Algiers, and about 80 km southeast of the city of Ouargla and 176 km south of Touggourt. While Hassi Messaoud is not among the top 10 largest oil fields globally, it is a major oil field in Africa and plays a critical role in Algeria's economy.

The giant Hassi Messaoud field (HMD), operated by Sonatrach, is one of the largest mature oil fields in the world. It was discovered in 1956 and began production in 1958. It covers an area of 3,300 square kilometers and contains 1,800 wells. The field is operated using gas flood and waterflood techniques. Gas lift is used in approximately 40% of oil production wells **Figure (I.1)**. Contributes for more than 50% of Algerian production.

The Hassi Messaoud field has historically produced around 1 million barrels per day (bpd) at its peak, primarily produces crude oil its typically medium to light grade with an API gravity ranging from 30° to 40°.

Additionally, it contains asphaltenes, which are a significant focus of research due to their tendency to cause deposition issues in production systems. Asphaltene Deposition are a common issue in Hassi Messaoud, leading to damage the formation (reservoir) and tubing or other surface facilities. [1]

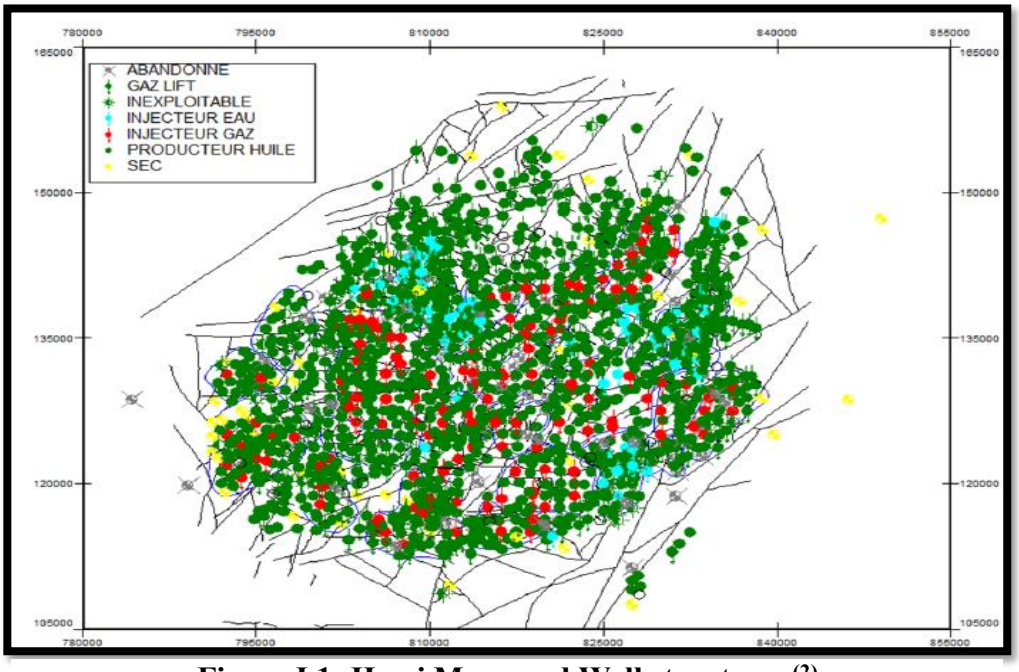

Figure I.1: Hassi Messaoud Well structure. [2]

I.2. Geographic Overview of Hassi Messaoud field:

Figure I.2: Hassi Messaoud (HMD) field location-Google earth map. [2]

I.2.1. geographic coordinates (HMD):

X = 790,000 - 840,000 Est,

Y = 110,000 - 150,000 North.

I.2.2. situation of the Hassi Messaoud:

the limited Hassi Messaoud reservoir:

- To the North-West by the Ouargla traps (Gellala, Ben Kahla and Houd Berkaoui).
- To the South- West by the traps of El-Gassi, Zotti and El Agreb.
- To the East by the Ghadames trap. [1]

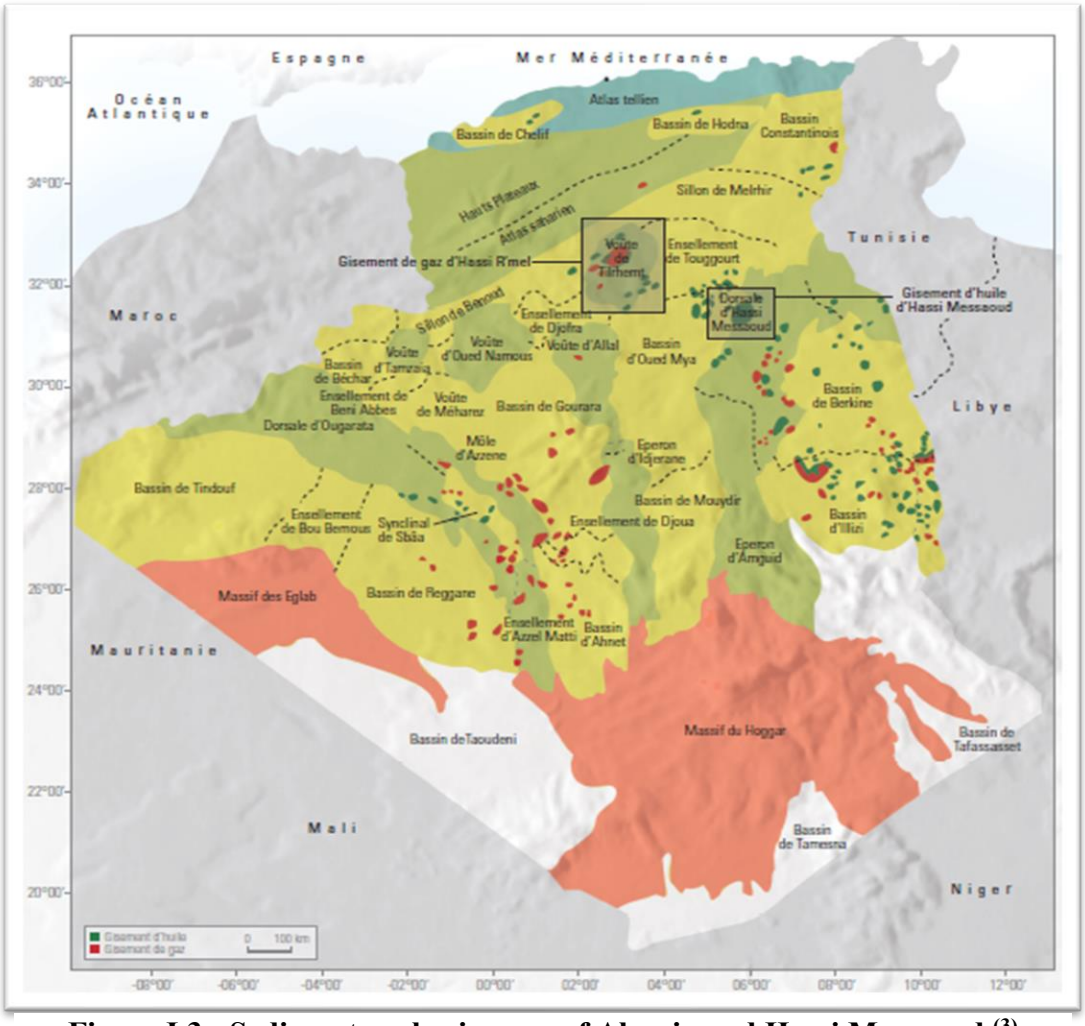

Figure I.3: Sedimentary basin map of Algeria and Hassi Messaoud [3]

I.3. Hassi Messaoud trap structure:

The Hassi Messaoud reservoir is a broad, gently folded anticline developed within Cambro-Ordovician sandstones. It is situated on a major regional structural axis trending NNE–SSW, which strongly influenced sedimentation processes up to the early Upper Cretaceous. This structural high played a key role in the migration and trapping of hydrocarbons, contributing to the formation of one of the largest oil accumulations in Algeria. The structure is asymmetrical, with a steeper western flank and a more gradual eastern slope, which also affects fluid distribution within the reservoir. Its tectonic stability over time has helped preserve the oil column and maintain reservoir continuity. [4]

I.4. lithostratigraphic log of the Hassi Messaoud reservoir:

Figure (I.4) present lithostratigraphic log of the Hassi Messaoud reservoir, combining gamma ray and neutron well log with sample images and lithological descriptions for each layer. it spans throw the main Cambrian units, including Ra, R2, and R3, which can be divided to many sedimentary layers such as D1 through D5 and R2a–c.

Zone Ri: or isometric sandstones, usually very compact: D5 or (R70 – R 90), subdivided into three sections.

The Ra zone: is the most important geologically. These layers show well-developed siliceous sandstones, Fine to medium grain sizes, moderate clay content, and visible sedimentary structures suggest good porosity and permeability, particularly in intervals D2 and D1 and ID.

The R2 zone: is quartzitic and argillaceous sandstones, with increased clay content and lower reservoir-quality intervals. This unit is generally more compact, with limited fluid flow potential. so, it's unlikely to favorable hydrocarbon storage.

The R3 unit: composed of very coarse sandstones and micro-conglomerates, is highly argillaceous with very limited reservoir capacity and low porosity, makes it unsuitable for hydrocarbon storage. [5]

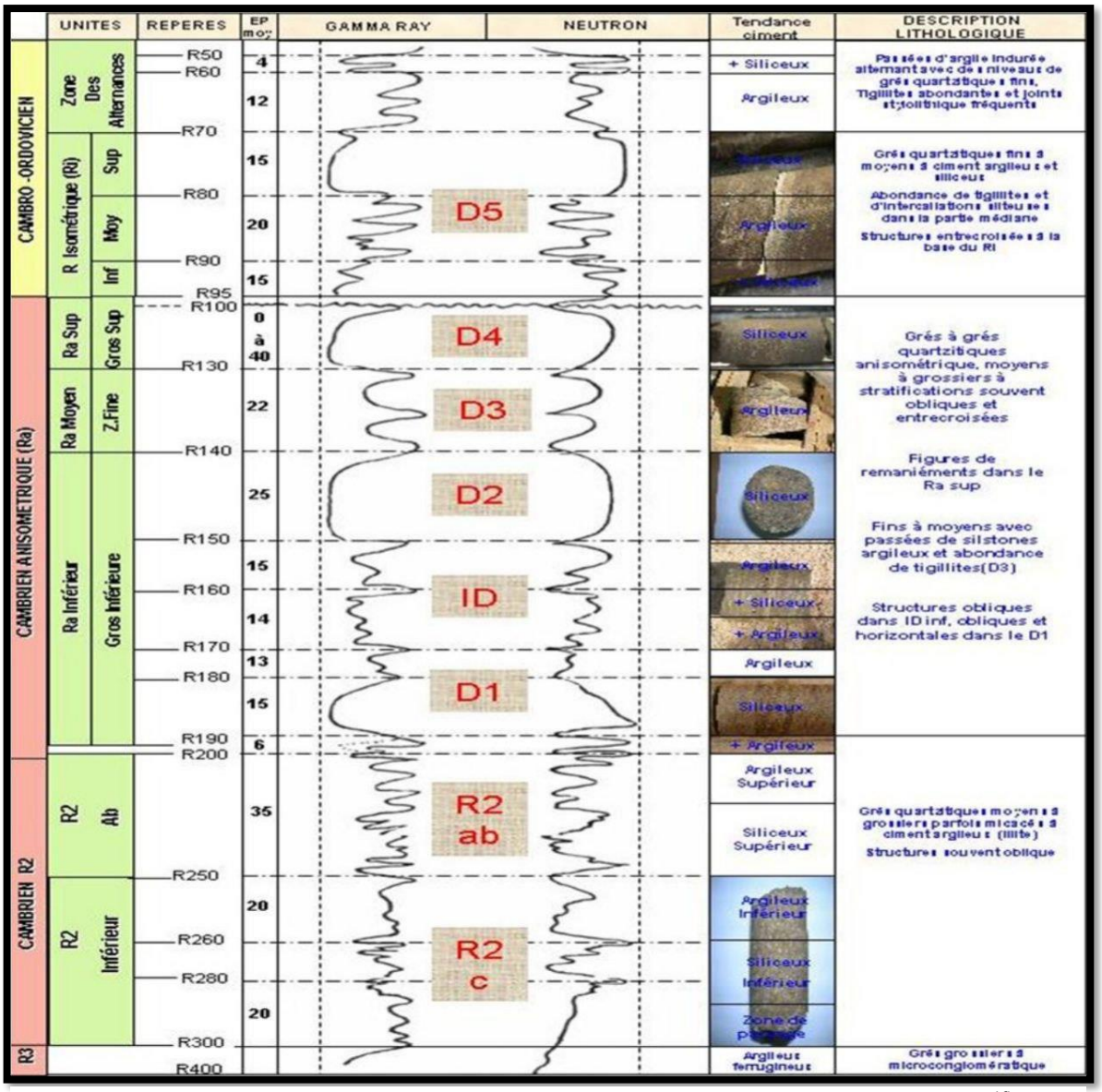

Figure I.4: Typical stratigraphic column of the Hassi Messaoud region. [6]

I.5. Main Problems in the Hassi Messaoud Field:

I.5.1. Reservoir Heterogeneity:

Two main factors explain the complexity are:

a. faulting and the erosion cause the local complications.
b. Diagenesis is tied to tectonics and caused the deterioration of the reservoir qualities.

I.5.2. Drain Contribution by Field Zone:

Different layers contribute to production depending on the field area:

- In the **central zone**, the main producing layers are D1, ID, and D2.
- On the **western side**, production comes from D4 and D5.

I.5.3. The production zones and pressure behavior:

The reservoir is currently divided into 25 production zones, separated by non-productive areas. This zoning was not based on geological features but on pressure behavior observed using numerical simulation tools.

In **Figure (I.5)**: the red frame encloses the area of interest. A system of 25 isolated zones having different petrophysical and pressure characteristics, can be identified within the reservoir. (7)

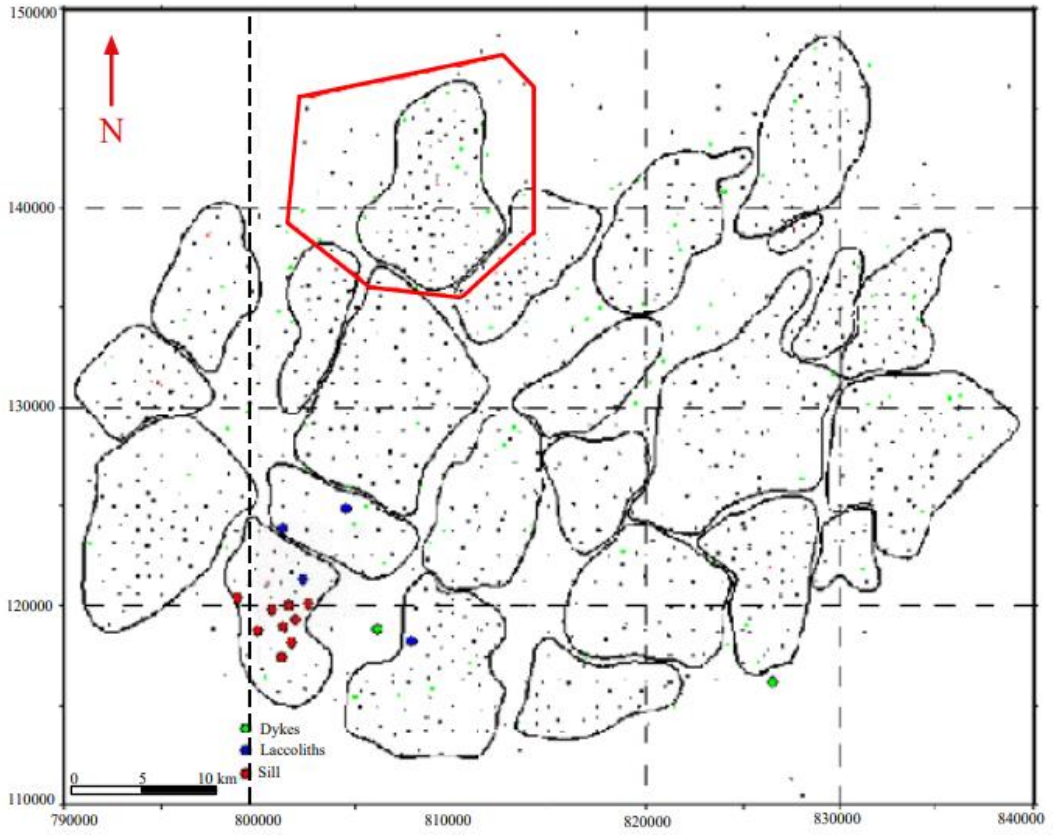

Figure I.5: examples of Intracambrian intrusions in the Southwest part of the Hassi Messaoud Field. (8)

I.5.4. Gaz injection:

Gas injection programs within producing zones show anisotropic fluid movement meaning the gas is moves unevenly.

In some situations, injected gas reaches nearby wells, and that complicate reservoir management.

I.5.5. Dry wells:

The plantation of 106 dry wells in the field is considered to be one of the negative points inexplicable by the present geological and reservoir models.

I.5.6. Asphaltene Deposition:

Causes formation damage by block reservoir and wellbore, tubing and surface facilities. [9]

Here are some examples of what the deposition of asphaltene will look like:

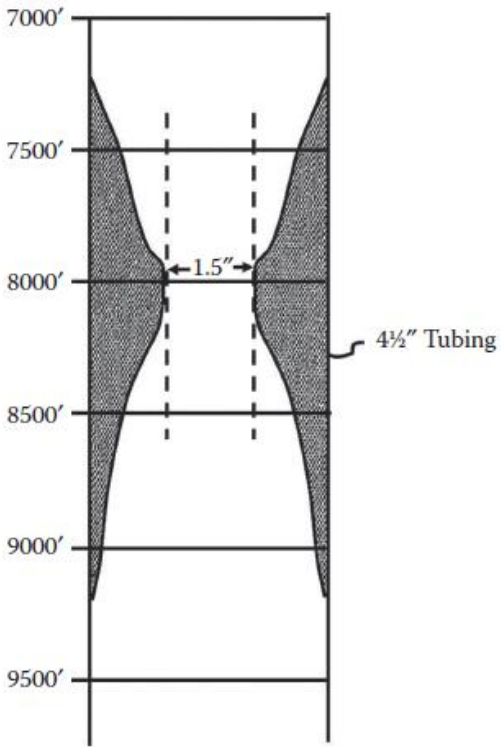

Figure I.6: Asphaltene deposition profile in one of Hassi Messaoud oil wells. [10]

The Asphaltene deposition in porous media is represented in **Figure (I.7)**

(a) Asphaltenes are dissolved in the oil phase.

(b) asphaltenes precipitate as a result of changes in oil pressure, temperature, or composition. They deposit in the porous media and plug the pore throats.

(c) some of the deposits are entrained by the oil flow.

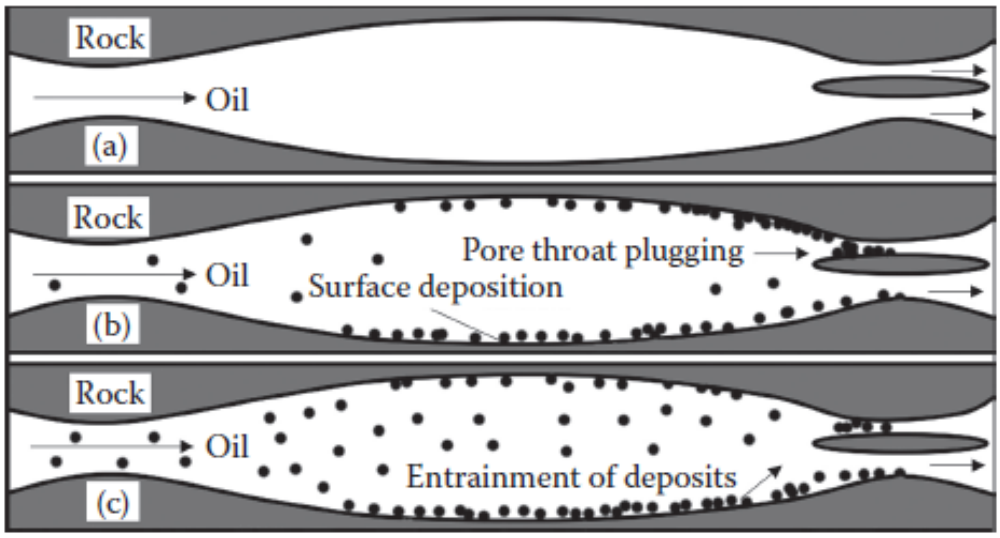

Figure I.7: Asphaltene deposition in porous media. [10]

I.6. Crude oil:

Crude oil is a natural liquid fossil fuel that is found in underground reservoirs. It's a mixture of hydrocarbons (compounds made of hydrogen and carbon) and small amounts of other substances like sulfur, nitrogen, and metals. it is one of the most important substances used by modern society .However, it remains one of the things that needs more research in order to understand it . Its behavior is directly related to its chemical composition and physical properties.

Each crude oil has a different composition depending on where it's extracted.it can be heavy or light, sweet or sour. And the fraction of the element in it can also changes, it is mainly used to make fuels and petrochemicals like: plastics, synthetic rubber.

I.7. Importance of Crude oil in the energy sector:

Crude oil remains a cornerstone of the global energy system, providing approximately 31% of the world's primary energy consumption. Its importance stems from several factors:

I.7.1. Energy Density:

Crude oil has a high energy content, making it an efficient fuel source for transportation, power generation, and industrial applications.

I.7.2. Versatility:

It serves as a feedstock for producing a wide range of products, including fuels, lubricants, plastics, and chemicals.

I.7.3. Economic Impact:

Crude oil is a major driver of economic growth, particularly in oil-exporting countries like Algeria. The Hassi Messaoud field alone accounts for nearly 70% of Algeria's crude oil production, underscoring its strategic significance.

However, the reliance on crude oil also presents challenges, such as environmental concerns, price volatility, and technical issues like asphaltene deposition. Addressing these challenges is essential for ensuring sustainable and efficient oil production. (11)

I.8. Crude Oil Definition and Classification:

It is classified based on its physical and chemical properties, primarily density and viscosity, into three main categories:

- **Light Crude Oil:** Characterized by low density and high API gravity (above 31.1° API). Light crude is easier to refine and yields a higher proportion of valuable products like gasoline and diesel.
- **Medium Crude Oil**: Falls between light and heavy crude in terms of density and API gravity (22.3°–31.1° API). It is widely used in refineries for producing a balanced mix of fuels and petrochemicals.
- **Heavy Crude Oil:** Has high density and low API gravity (below 22.3° API). Heavy crude is more viscous and contains higher concentrations of asphaltenes and other heavy components, making it challenging to extract and process.

Classifying crude oil is important to know its price and how to refine it. [12]

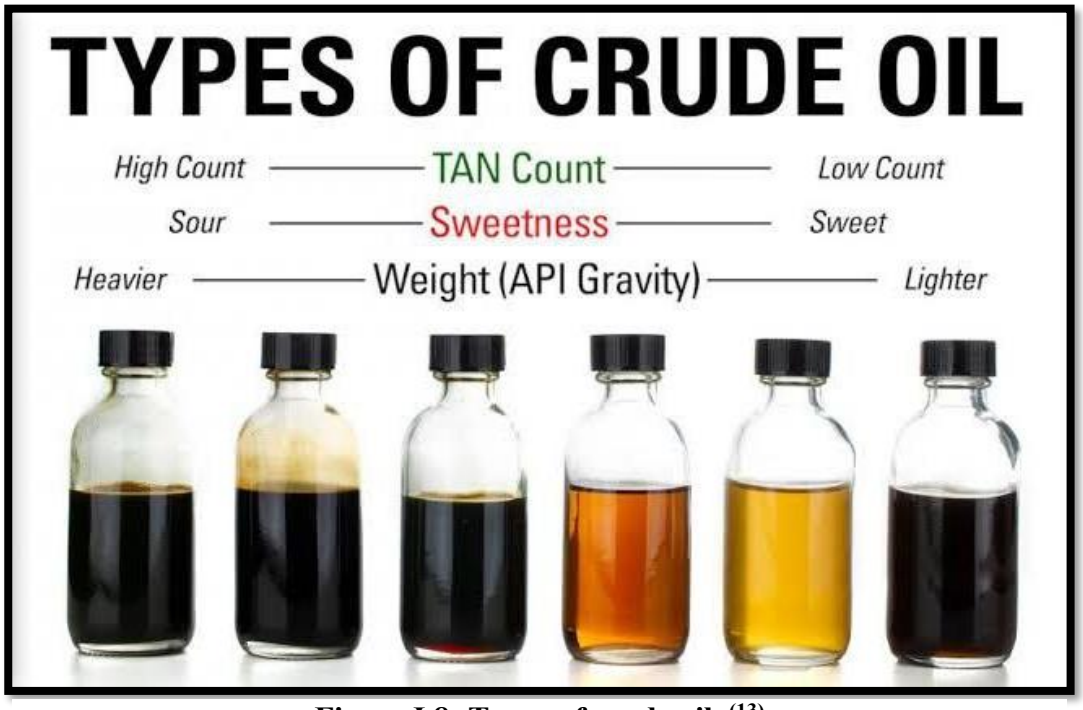

Figure I.8: Types of crude oil. [13]

I.9. Chemical Composition:

hydrocarbons can be broadly categorized into two groups:

I.9.1. Hydrocarbons components:

- **Aliphatic Hydrocarbons:** Linear or branched chains of carbon atoms, including paraffins (alkanes) and olefins (alkenes). Aliphatic are typically lighter and more volatile (light).
- **Aromatic Hydrocarbons:** These have ring-shaped structures with alternating single and double bonds, like benzene and naphthalene. They are heavier and play a role in forming asphaltenes.

I.9.2. non-hydrocarbon components:

- **Sulfur Compounds:** Present as organic sulfides, thiophenes, or elemental sulfur. High sulfur content increases refining complexity and environmental concerns.
- **Nitrogen and Oxygen Compounds:** Found in small quantities but can significantly affect crude oil stability and processing.

- **Trace Metals:** Such as nickel, vanadium, and iron, which are often associated with asphaltenes and can catalyze undesirable reactions during refining.

The chemical makeup of crude oil affects how it behaves during production, transport, and refining. For example, heavy crude oils with a lot of asphaltenes are more likely to cause deposition problems, especially when pressure or temperature changes. [12]

I.10. Crude oil properties:

Crude oil is a liquid mixture composed primarily of carbon and hydrogen, with smaller amounts of oxygen, nitrogen, sulfur, and trace heavy metals such as nickel, vanadium, copper, cadmium, and lead. These heavy metals are assumed to have acted as catalysts in petroleum formation.

I.10.1. Density and API Gravity:

API gravity is created by The American Petroleum Institute to measurement (°API)

API gravity = (141.5/d) - 131.5 at 60°F

In this scale, water has an API gravity of **10°.**

Density (ρ): is defined as mass per unit volume (kg/m³) and is a state function dependent on temperature and pressure. Crude oil density decreases with increasing temperature, while pressure effects are usually negligible at moderate pressures (less than a few bars). At higher pressures, density increases as volume decreases.

Based on density, crude oils are classified into four grades:

Light: $\rho < 870$ kg/m³; API > 31.1°

Medium: $870 < \rho < 920$ kg/m³; 22.3° < API < 31.1°

Heavy: $920 < \rho < 1000$ kg/m³; 10° < API < 22.3°

Extra heavy: $\rho > 1000$ kg/m³; API < 10°

Density can be determined using the following tools:

hydrometers (**ASTM D287**, **ASTM D1217**) or pycnometers (**ASTM D1298**).

I.10.2. Viscosity:

Viscosity measures a fluid's resistance to deformation by shear or tensile stress—essentially, its internal resistance to flow. This property is crucial for designing appropriate extraction processes, transport systems, and planning remediation measures in case of spills, Crude oil viscosity change depending on the composition specially the heavy ones.

I.10.3. Molecular Weight:

The molecular weight of crude oil is usually from 200 to 300 g/mol, although heavier oils can exceed 400 g/mol. This property is very important for characterization.

I.10.4. Water content:

sins Crude oil is mixture it is naturally contains some water, around 0.02% to 0.2% of total weight. Water content affects processing, transportation, and refining operations. Excessive water can cause corrosion in pipelines and equipment.

Water content is commonly measured using the Karl Fischer titration method or through distillation techniques as specified in ASTM standards.

I.10.5. Solubility Parameter:

The solubility parameter helps predict how crude oil components will interact with solvents and with each other. This parameter is particularly important for understanding asphaltene behavior, like precipitation and Aggregation and deposition because it is directly linked to solubility interactions between asphaltene and the rest of the components.

I.11. Crude Oil Fractionation:

Crude oil can be fractionated based on different criteria:

I.11.1. Based on Boiling Point:

Distillation separates crude oil into fractions with different boiling point ranges, including gases, naphtha, kerosene, gas oil, and residue.

I.11.2. Based on Chemical Structure:

Crude oil components can be classified as paraffins (alkanes), naphthenes (cycloalkanes), aromatics, and non-hydrocarbons (containing S, N, O, and metals).

I.11.3. Based on Polarity:

Which can be called The SARA (Saturates, Aromatics, Resins, Asphaltenes) analysis separates crude oil based on component polarity and solubility. This method is particularly important for understanding asphaltene behavior and predicting deposition issues, and it's the most used and effective one. [10]

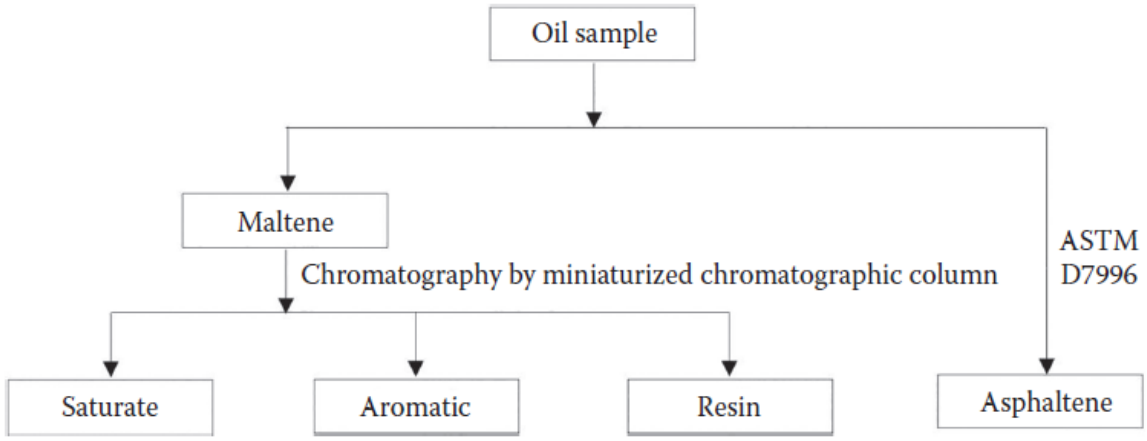

Figure I.9: Maze method for SARA analysis. [10]

The maltene passes through the mini-column and the mobile phase, which the solvent washes the column continually. Saturates content is calculated by measuring the refractive index of the sample. For resins and aromatics, the optical absorbance is measured by a spectrometer to find the content of each fraction. The advantages of this new method are that it is automated and the results are repeatable and reproducible.

We can say that this is the main method used to distract the asphaltene from crude oil.

I.12. Deposition Problems in Oil and Gas Wells:

Deposition problems are among the most significant challenges in oil and gas production, particularly in Hassi Messaoud. These issues arise due to changes in pressure, temperature, and composition during extraction and transportation. Deposition can be divided to two types mainly:

I.12.1. Organic Deposits:

There is multiple organic deposition like:

- Asphaltenes are complex, heavy molecules found in crude oil, they can precipitate (come out of solution) when there's a change in pressure, temperature, or the type of solvent in the oil. Asphaltenes are one of the main reasons for flow problems, especially in heavy oil fields.

- Waxes are long-chain hydrocarbons (also called paraffins) that can harden at low temperatures, when this happens, they form waxy layers in the wellbores or pipelines or both, Wax deposits are usually found in light and medium crude oils.

Figure I.11: Asphaltene deposition. [14]

Figure I.10: Wax deposition. [15]

I.12.2. Inorganic Deposits:

There are multiple inorganic deposition like:

- Scale: Mineral deposits, such as calcium carbonate ($CaCO_3$) and barium sulfate ($BaSO_4$), that form due to chemical reactions between water of injection and formation.

- Hydrates: Ice-like crystalline structures formed by water and natural gas molecules under high-pressure and low-temperature conditions. (16)

Figure I.13: Scale deposition. (17)

Figure I.12: Hydrates deposition. (18)

I.13. What is the asphaltene:

Asphaltenes are complex, high-molecular-weight hydrocarbons made of fused aromatic rings with alkanes ending. They are the heaviest and most polar fraction of crude oil.

Polarity in chemistry refers to how electrically reactive a molecule is. They contain atoms like nitrogen, sulfur, and oxygen, which make them more chemically active and sticky.

So, what that mean is: because of this polarity, asphaltenes tend to interact with rock surfaces, form stable emulsions, and cause deposits when conditions change. (12)

They are among the most complex components of crude oil, characterized by their insolubility in light alkanes (e.g., n-pentane or n-heptane) but solubility in aromatic solvents such as toluene. They are composed of high-molecular-weight hydrocarbons with a significant presence of heteroatoms (sulfur, nitrogen, and oxygen) and trace metals (nickel and vanadium).

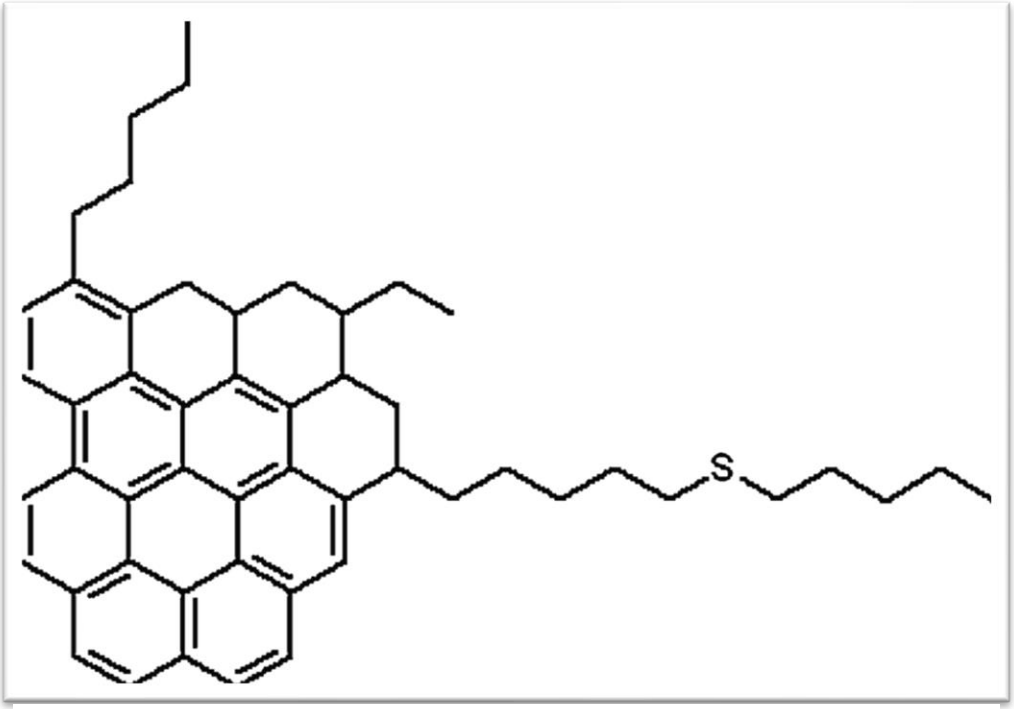

Figure I.14: the structure of the Asphaltene in generale. [10]

I.14. precipitation, aggregation, and aging:

The asphaltene are special cause of their mechanism of precipitation, aggregation, and aging.

which is the process when asphaltene particles started to stick together to form larger clusters due to interactions such as π–π stacking between aromatic rings. cause of the drop in pressure or temperature. [10]

This behave is explained in the **Figure** (II.8):

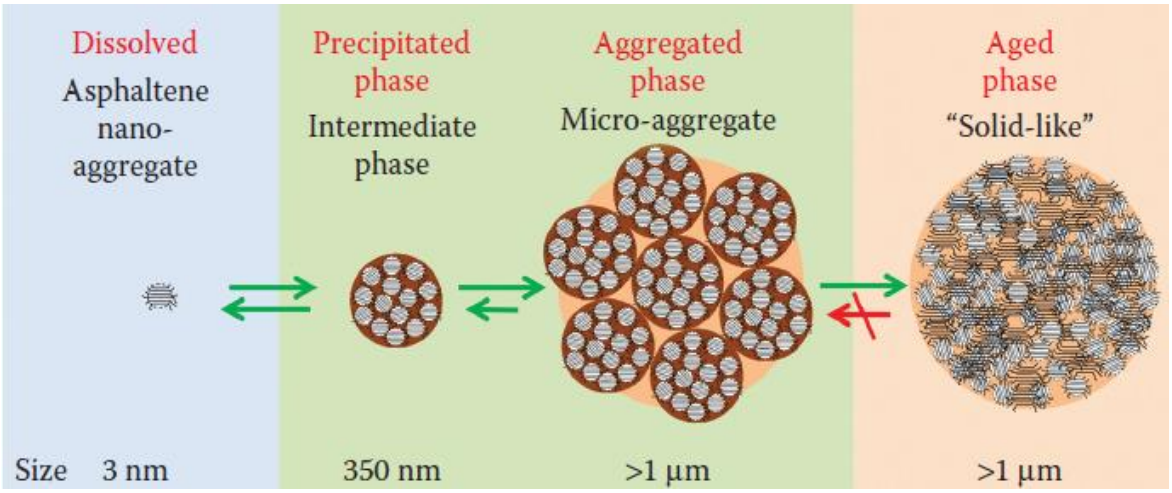

Figure I.15: Proposed multistep mechanism for asphaltene precipitation, aggregation, and aging. [10]

As we can see, it's divided to 4 main sections:

I.14.1. Dissolved Phase:

In this phase, asphaltenes exist in **dissolved** form as liquid, usually as **nano-aggregates (3nm)**, these particles are stable in crude oil due to the **solvent power** of resins and maltenes.

I.14.2. Precipitated Phase:

When pressure, temperature, or composition changes, asphaltenes precipitate out of solution, and form intermediate-size particles (350 nm).

I.14.3. Aggregated Phase:

Precipitated particles start to cluster together, forming larger micro-aggregates, these clusters are bigger than (1µm).

I.14.4. Aged Phase:

Over time, micro-aggregates become more compact and organized so they look more like a solid, structures are hard to break apart and are thermodynamically stable, this can cause permanent deposition all over the well (in reservoir or tubing or pipelines or surface facility).

Note: In the first 3 phases the this behave is still reversible, but when it reach the aged phase its irreversible and Chemical inhibitors are needed.

I.15. Asphaltene Precipitation Diagram:

When the oil flows from the reservoir to the surface, it undergoes changes in pressure and temperature. In the reservoir, the oil is typically in a single liquid phase under high pressure and high temperature and as it moves upward through the production tubing, both pressure and temperature begin to drop, this drop in pressure causes the oil to swell, due to the expansion of its light hydrocarbon components.

Since asphaltenes are the heaviest and most complex molecules in the crude oil, they are insoluble in these lighter components. As the oil becomes richer in expanded light fractions, it turns into a poor solvent for asphaltenes and when this happened, the asphaltenes start to precipitate out of the oil and form a separate solid like phase **Figure (II.8)**. This first visible point of asphaltene appearance is known as the Asphaltene Onset Pressure (AOP) — labeled as point A in the diagram, **Figure (II.9. (b)).**

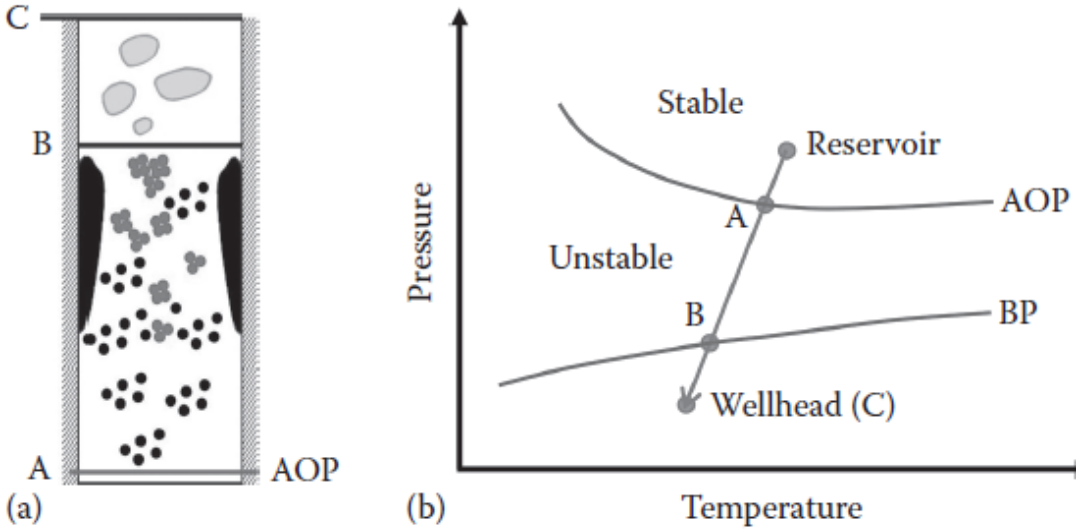

Figure I.16: (a) Schematic of asphaltene precipitation, aggregation, and deposition in wellbore, (b) (P-T) diagram for an oil sample being produced from an underground reservoir. AOP, asphaltene onset pressure; BP, bubble point. [10]

As the oil continues to flow toward the surface, pressure keeps decreasing and more light fractions expand, causing more asphaltenes to precipitate (the oil moves from point A to point B). When the oil reaches the bubble point (BP) labeled as point B the light hydrocarbons begin to vaporize, leaving behind a heavier liquid. This heavier liquid is a

better solvent for asphaltenes, which allows some of the previously precipitated asphaltenes to redissolve into the oil.

Note: In some cases, by the time the oil reaches the wellhead, all the asphaltenes may have redissolved, and no deposits are observed at surface conditions.

Asphaltene precipitation can begin inside the reservoir before the oil even enters the production tubing especially: In depleted reservoirs (low pressure from primary depletion).

During miscible gas injection operations like (CO_2 or N_2), where injected gases reduce oil's solvent power, leading to precipitation within the porous rock and that's why the highest risk of asphaltene precipitation occurs around the bubble point, and managing pressure profiles is critical for flow assurance and formation damage prevention. [10]

Chapter II: Asphaltene characterization, composition and structure.

II.1. Introduction:

As we have said earlier in the previous chapter Asphaltene are the heaviest and most complex fraction of crude oil, they are a polydisperse mixture defined by their solubility behavior rather than by a specific chemical composition. They are insoluble in light paraffinic solvents (such as n-pentane or n-heptane) but soluble in aromatic solvents (such as toluene or benzene). This operational definition means that asphaltenes from different sources can have significantly different chemical characteristics despite similar solubility behavior.

Understanding their composition and structure is crucial for predicting and mitigating deposition problems.

Mainly there are two structure model that asphaltene follow: the **Island** model and **Archipelago** model, Recent research using advanced analytical techniques suggests that the island structure is predominant in most asphaltenes, though some may exhibit archipelago characteristics.

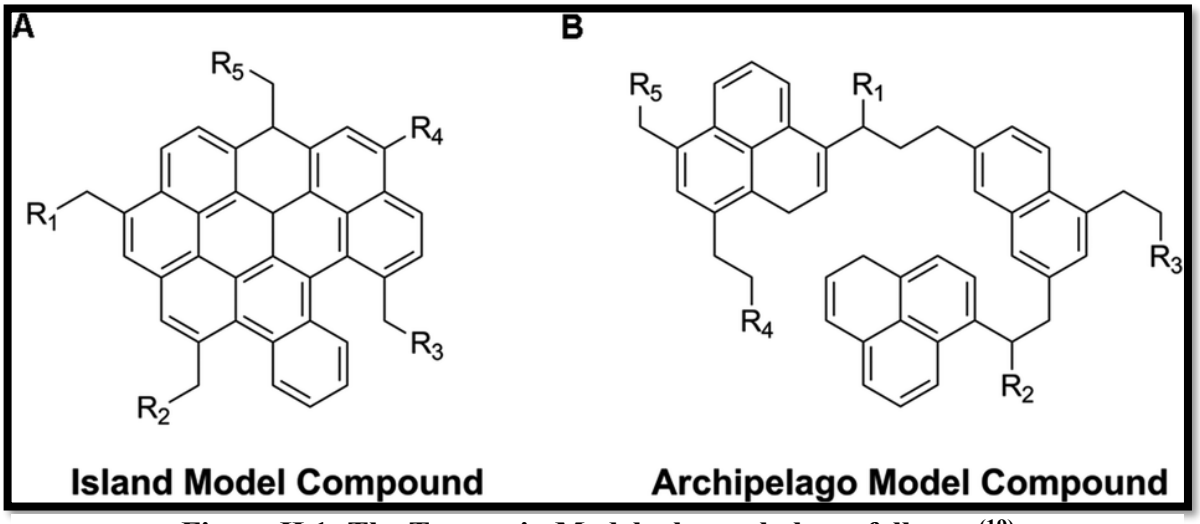

Figure II.1: The Two main Models the asphaltene follows. [19]

Island Model:

A single large polyaromatic core with peripheral aliphatic chains.

Archipelago Model:

Multiple smaller aromatic clusters connected by alkyl bridges.

II.2. Asphaltene composition and chemical structure:

To determinate Asphaltenes composition or molecular structure we need a characterization process that contain several deferent analyses, because Asphaltenes are defined by their solubility, not by exact molecular identity.

Despite having similar solubility, asphaltenes can contain thousands of different molecules, with over 10^5 unique species identified. There for a wide range of analytical methods are used to study their composition, structure and decomposition behavior.

II.3. Determination Elemental composition:

The elemental composition of asphaltenes provides fundamental insights into their structure, behavior, and potential problems they might cause during oil production and processing. Asphaltenes typically contain by weight:

Carbon: 80-86%

Hydrogen: 7-12%

Nitrogen: 0.2-1.5%

Oxygen: 0.3-4.9%

Sulfur: 1.5-8.5%

Metals: Primarily vanadium (up to 1580 ppm) and nickel (up to 340 ppm). [10]

The hydrogen-to-carbon (H/C) atomic ratio is a particularly important parameter, typically ranging from 1.0 to 1.2 for asphaltenes. This ratio serves as an indicator of aromaticity lower H/C ratios indicate higher aromaticity and more condensed ring structures. Furthermore, n-heptane insoluble asphaltenes (C7+) generally have lower H/C ratios and higher heteroatom content than n-pentane insoluble asphaltenes (C5+), indicating they are less paraffinic, heavier, and more polar. [20]

II.3.1. Elemental analysis:

The elemental analysis is Several analytical techniques that employed to determine the elemental composition of asphaltenes:

II.3.1.1. CHNS Analysis:

Combustion-based methods determine carbon, hydrogen, nitrogen, and sulfur content (C, H, N, S). The sample is completely oxidized at high temperatures (typically 900-1100°C) in an

oxygen-rich environment. The combustion products (CO_2, H_2O, N_2, and SO_2) are separated and quantified using gas chromatography or infrared spectroscopy.

Oxygen Determination: Oxygen content is often determined by difference (subtracting the sum of all other elements from 100%) or by specialized pyrolysis techniques where oxygen is converted to carbon monoxide and measured.

II.3.1.2. Metals Analysis:

Inductively Coupled Plasma (ICP) techniques, including ICP-Mass Spectrometry (ICP-MS) and ICP-Optical Emission Spectroscopy (ICP-OES), are used to determine metal content. These methods involve sample digestion in strong acids followed by atomization and ionization in a plasma torch.

II.3.1.3. X-Ray Fluorescence (XRF):

This non-destructive technique can determine elemental composition by measuring the fluorescent X-rays emitted when the sample is excited by a primary X-ray source.

The distribution of heteroatoms within the asphaltene structure provides important insights:

Nitrogen: Usually exists in aromatic structures as pyrrolic nitrogen (most common) and pyridinic nitrogen.

Oxygen: Can be founded in various functional groups including aliphatic hydroxyl groups, ketones, quinones, ethers, esters, and carboxylic acids.

Sulfur: Most commonly present in thiophenes, sulfides, and sulfoxides.

Metals: Exist as porphyrins (organometallic complexes) or as high molecular weight complexes associated with asphaltenes.

II.4. Determination of Chemical Structure:

A Several complementary analytical techniques are used to elucidate the complex molecular architecture of asphaltenes:

II.4.1. Fourier Transform Infrared (FTIR) Spectroscopy:

FTIR spectroscopy identifies functional groups in asphaltenes by measuring the absorption of mid-infrared radiation (wavelengths between 2.5 μm and 25 μm). When exposed to infrared radiation, chemical bonds in the molecule selectively absorb radiation of specific wavelengths, changing their dipole moment and vibrational state.

The FTIR spectrum of asphaltenes typically shows several characteristic absorption bands:

- 2950-2850 cm^{-1}: C-H stretching in alkanes (CH_3 and CH_2 groups)
- 1600 cm^{-1}: C=C stretching in aromatic rings
- 1470-1350 cm^{-1}: C-H bending in alkanes
- 1030-1200 cm^{-1}: C-O stretching in alcohols, ethers, and esters
- 700-900 cm^{-1}: Out-of-plane C-H bending in aromatic rings

In summary FTIR analysis provides valuable information about:

- The ratio of aliphatic to aromatic structures
- The presence and relative abundance of heteroatom-containing functional groups

The degree of condensation in polyaromatic compounds. [10]

Figure II.2: Fourier Transform Infrared (FTIR) Spectrometer – Thermo Scientific System. [21]

II.4.2. Nuclear Magnetic Resonance (NMR) Spectroscopy:

NMR Spectroscopy is one of the most powerful techniques for determining asphaltene structure. It provides detailed information about the carbon skeleton and hydrogen distribution by measuring the magnetic properties of certain atomic nuclei.

^1H NMR identifies different types of hydrogen atoms in asphaltenes:

Aromatic hydrogens (6.5-9.0 ppm)

Hydrogens attached to carbons adjacent to aromatic rings (2.0-4.0 ppm)

Hydrogens in methyl and methylene groups in aliphatic chains (0.5-2.0 ppm)

^{13}C NMR provides information about carbon types:

- Aromatic carbons (110-160 ppm)
- Aliphatic carbons (10-60 ppm)
- Carbonyl carbons (170-210 ppm)

Advanced NMR techniques such as 2D correlation spectroscopy (COSY, HSQC, HMBC) can establish connectivity between different atoms, helping to build a more complete structural image. (10)

II.4.3. X-ray Diffraction (XRD):

XRD analysis provides information about the stacking of aromatic sheets in asphaltenes. From the difference pattern

X ray Diffraction (XRD) is a technique that uses X-rays to look at how atoms are arranged in a material. When the atoms are in an ordered, repeating pattern, the X-rays bounce off them in a specific way. This interaction is described by a simple rule called Bragg's.

II.5. Lab experiment using (XRD) on Zone 01 samples:

When X-rays hit the sample, they are diffracted by the ordered structures. The stacked aromatic sheets act like layers in a crystal lattice, diffracting X-rays at specific angles according to **Bragg's** Law (Figure III.3):

$$n\lambda = 2d\,sin(\theta) \qquad \text{II-1}$$

- **d:** interlayer spacing (is the distance between the layers of atoms) (in Å: angstroms)
- **λ:** X-ray wavelength (for our machine, it is 1.5406 Å).
- **θ:** diffraction angle (the angle at which the X-rays hit the layers).
- n: is an integer

The XRD pattern of asphaltenes typically shows a broad peak around $2\theta \approx 25\text{-}26°$ (using Cu Kα radiation, $\lambda \approx 1.54$ Å).

This peak is known as the (002) peak that representing the diffraction from the stacked aromatic layers. (22)

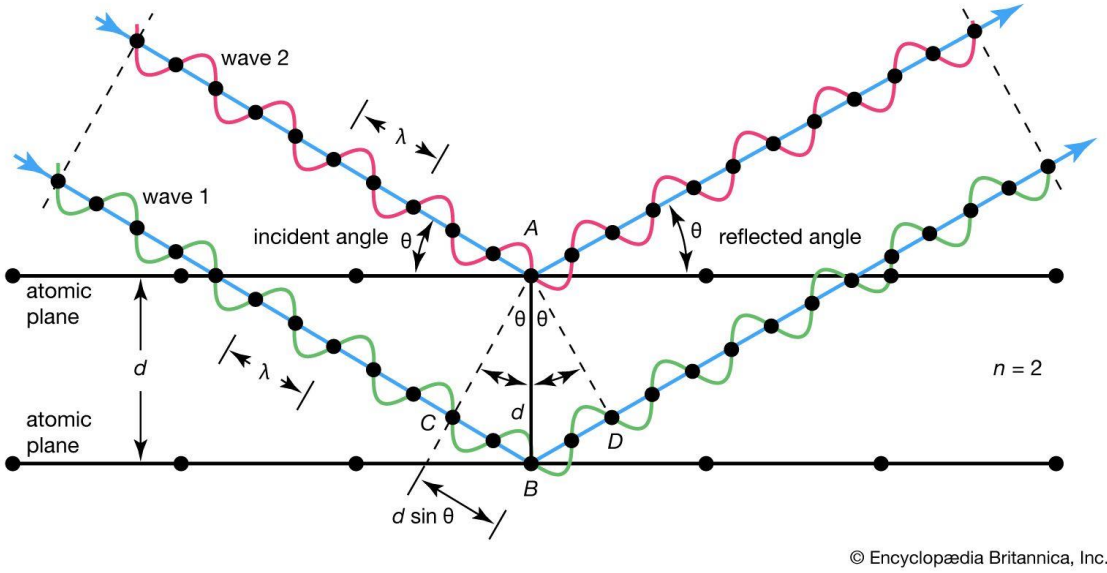

Figure II.3: A diagram showing how Bragg's Law works. X-rays hit the atomic layers and bounce off. [23]

II.5.1. XRD Apparatus:

To get the data, we use a machine called an X-ray diffractometer (Figure III.4). This machine shoots a beam of X-rays at our asphaltene sample. A special detector then moves around the sample to measure the intensity of the X-rays that bounce off at different angles (2θ). The result is a graph that shows intensity versus angle, which is the XRD pattern we analyze. [13]

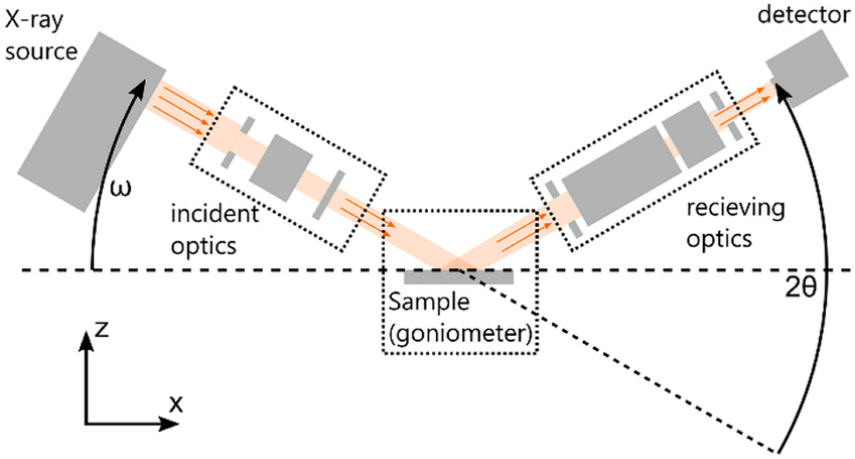

Figure II.4: The main parts of an X-ray diffractometer. [24]

Figure II.5: A picture showing the exterior of the XRD apparatus.

II.5.1.1. How to Read an XRD Pattern: Sharp Peaks vs. Wide Humps:

When we look at an XRD pattern, the shape of the peaks tells us a lot:

- Materials with a very organized, repeating structure (like a crystal) create a sharp, narrow peaks.
- Materials with a messy, disorganized structure called amorphous materials) create wide, broad humps, or" halos".

This idea is very important for understanding asphaltenes because their XRD patterns are a mix of both types of features, as shown in (Figure III.7). The sharp peaks we see in our samples come from the waxy parts (paraffins), which have a crystal-like structure. The wide humps come from the aromatic sheets, which are stacked on top of each other in a less organized way. (13)

II.5.1.2. Structural Parameters of Asphaltenes Derived from XRD:

We use the XRD patterns to calculate several key numbers that describe the asphaltene structure (**Figure III.6**):

- d-spacing (d): Represents the interplanar distance between parallel atomic or molecular layers. In asphaltenes, specific d-spacings are of particular interest:
- d002 (dm): The average interlayer spacing between stacked aromatic sheets. A larger d002 value suggests increased separation between these sheets, potentially due to the

intercalation of aliphatic chains.

- **daliphatic (dr):** The average spacing between aliphatic side chains.
- **Lc(Crystallite Height):** Denotes the average height of stacked aromatic sheets, indicating the number of aromatic layers piled vertically.
- **The (Crystallite Diameter):** Represents the average lateral dimension or diameter of a single aromatic sheet, providing an estimate of the extent of the aromatic core.
- **M (The average number of sheets in one stack):** We calculate it using M = Lc/d002.
- **Ra(Number of Aromatic Rings):** An estimation of the average number of aromatic rings within a single aromatic sheet, derived from the La value.
- **Fa(Aromaticity Factor):** Represents the fraction of carbon atoms that are part of aromatic structures. It is important to note that Fa cannot be directly determined from standard XRD peak analysis. Its determination typically requires complementary analytical techniques such as elemental analysis, Nuclear Magnetic Resonance (NMR), or X-ray Photoelectron Spectroscopy (XPS).

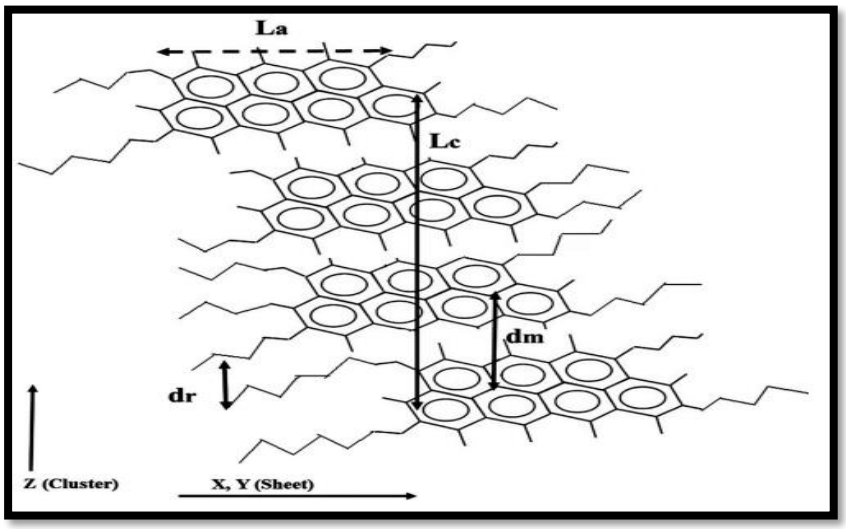

Figure II.6: A simple model of an asphaltene cluster, showing some structural parameters we measure with XRD. [25]

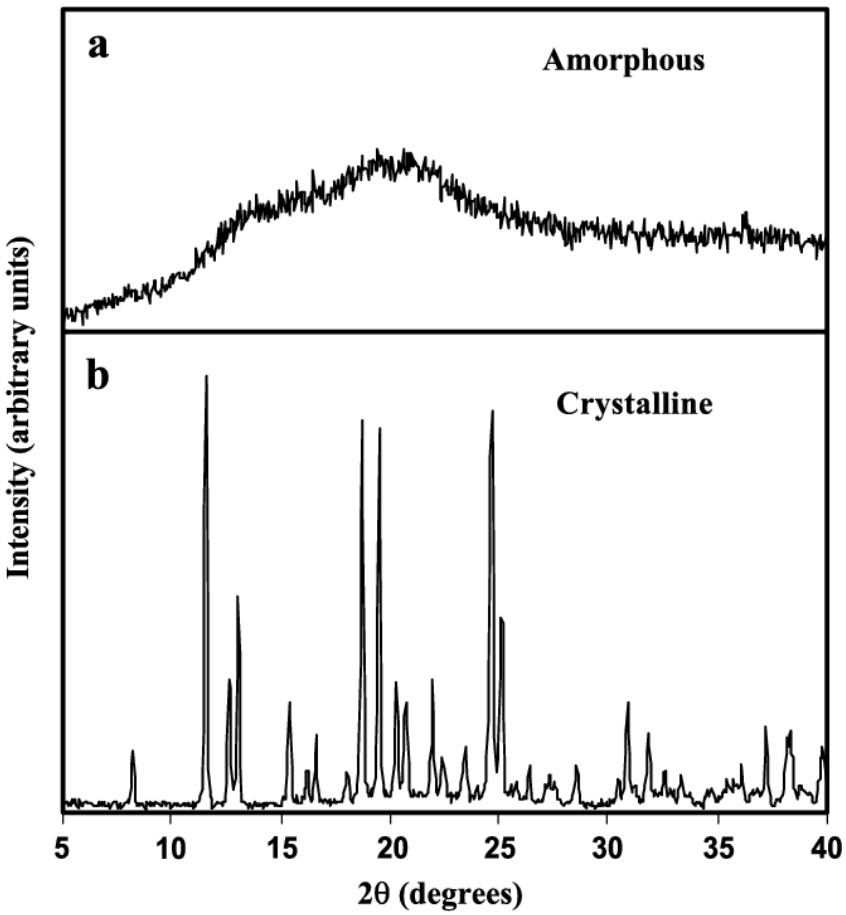

Figure II.7: A comparison of XRD patterns: (a) an amorphous material with a wide hump and (b) a crystalline material with sharp peaks. [26]

II.5.1.3. Full Width at Half Maximum (FWHM):

FWHM is a critical parameter extracted from diffraction peaks, providing information about crystallite size and structural perfection. It is defined as the width of the diffraction peak at half of its maximum intensity.

A narrower **FWHM** indicates larger and more perfectly ordered crystallites, while a broader **FWHM** suggests smaller crystallites or increased structural disorder.

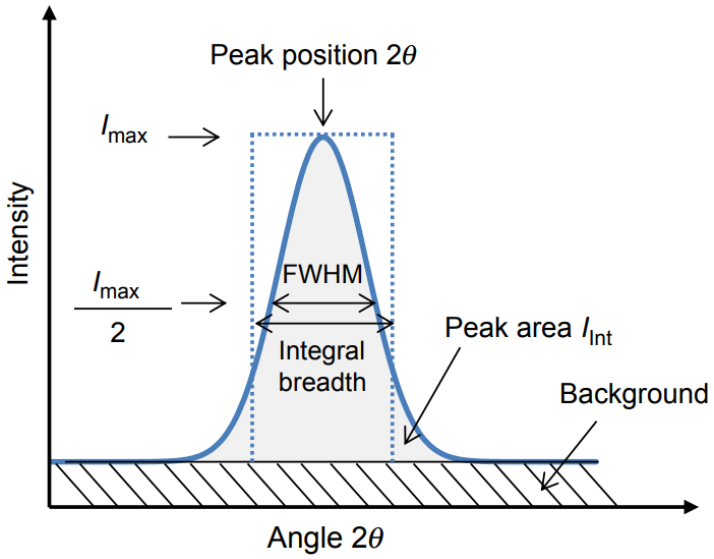

Figure II.8: Illustration of Full Width at Half Maximum (FWHM) on a diffraction peak. [27]

II.6. Experimental Methodology:

In this chapter, sample preparation and the X-ray diffraction (XRD) measuring procedure is outlined. Two samples, the third and the fourth, from a given sequence of samples, were measured. These two samples were both prepared and measured with the same conditions in order to be able to compare them with each other.

II.6.1. Sample Preparation

The samples in solid form were prepped for the analysis as per a standard procedure. First, each sample was powdered into a fine powder with the aid of a proper instrument. The collected powder was sieved through to gain a homogeneous and fine particle size, which is a prime parameter in obtaining quality diffraction data. A tiny amount of sieved powder was tightly packed into a specialty sample holder to form a flat and even surface for examination.

II.6.2. X-ray Diffraction (XRD) Analysis

The samples thus prepared were scanned with a BTX-716 X-ray diffractometer. It was configured with a Copper (Cu Kα) X-ray source. Significant measuring parameters for both samples remained the same:

II.6.2.1. Integration Time and step:

Data for a total of 2500 seconds for every sample was collected in order to achieve a satisfactory signal-to-noise ratio. The step was 0.05 degree

II.6.2.2. Geometry:

The sample was held in a constant geometry with the primary sensor angle at -30.346 degrees.

II.6.3. Data Processing:

The raw diffraction data were stored as a text file (.txt) for every sample. Data were opened in OriginPro (OriginLab) software for plotting and quantitative evaluation. The software was also utilized to plot the diffraction patterns and automatically quantify the selected peak parameters, such as the height, and the Full Width at Half Maximum (FWHM) using functions built in the software.

II.7. Results for Hassi Messaoud Asphaltenes lab experiment:

II.7.1. Results for the 3rd Asphaltene Sample:

Figure (III.9): shows the XRD pattern for the 3rd sample. We can see a very strong and sharp peak around $2\theta = 14.0^{\circ}$, which comes from the waxy material.

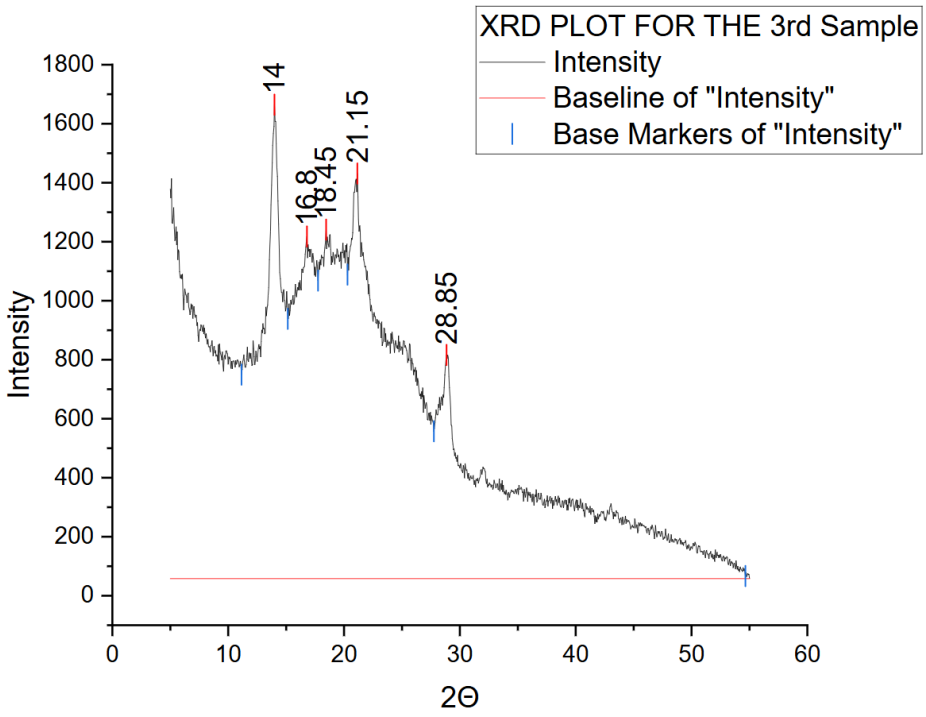

Figure II.9:XRD pattern for 3th Asphaltene Sample.

From this pattern, we calculated these key values:

• Distance between waxy chains (d paraffin):

The peak is at 2θ ≈ 14.0◦, so θ ≈ 7.00◦.

7.00 × (π/180) ≈ 0.1222 radians

$$d\,paraffin = \frac{\lambda}{2\,sin(\theta)} = \frac{1.5406\ \text{Å}}{2\,sin(7.00\ ^\circ)} \approx 6.32\text{Å} \qquad \text{II-2}$$

• Distance for other side chains (dr = dγ):

The peak is at 2θ ≈ 18.45 ◦, so θ ≈ 9.225 ◦.

9.225 × (π/180) ≈ 0.1610 radians

$$\mathbf{d\gamma} = \frac{\lambda}{2\ \sin\ (\theta)} = \frac{1.5406\text{Å}}{2\ \sin\ (9.5\ ^\circ)} \approx 4.81\ \text{Å} \qquad \text{II-3}$$

• Distance between aromatic sheets (dm=d002):

The peak is at 2θ ≈ 21.15 ◦, so θ ≈ 10.575 ◦.

10.575 × (π/180) ≈ 0.1846 radians

$$\mathbf{d002} = \frac{\lambda}{2\ \sin\ (\theta)} = \frac{1.5406\text{Å}}{2\ \sin\ (11.1\ ^\circ)} \approx 4.20\text{Å} \qquad \text{II-4}$$

• Average width of aromatic sheets (L_a):

Initial conversion of FWHM and 2θ values from degrees to radians is required:

• $\omega 10$ (FWHM in radians) = 5.880° ×(π/180) ≈ 0.1026 radians

• $\theta 10$ (half of 2θ in radians) = (21.15/2) × (π/180) = 10.575 × (π/180) ≈ 0.1846 radians

$$La = \frac{1.84\lambda}{\omega \cos \theta_{10}} \approx 28.10\ \text{Å} \qquad \text{II-5}$$

• **Average height of aromatic stack (L_c):**

$$Lc = \frac{0.9\lambda}{\omega \cos \theta_{002}} \approx 13.74\ \text{Å} \qquad \text{II-6}$$

• **Average number of sheets per stack (M):**

$$M = \frac{L_C}{d_{002}} = \frac{22,8A^0}{4.00A^0} \approx 5.7 \text{ sheets} \qquad \text{II-7}$$

• **Number of Aromatic Rings (Ra):** Ra is estimated using the calculated La value:

$$R_a = \frac{La}{3,35A^o} - 1 = \frac{28,10A^o}{3,35A^o} - 1 = 8.388 - 1 \approx 7.39 \qquad \text{II-8}$$

II.7.2. Results for the 4th Asphaltene Sample:

Figure (III.10) shows the pattern for the 4th sample. It also has a strong, sharp peak from waxy material, but at a slightly different position (2θ ≈ 14.5◦).

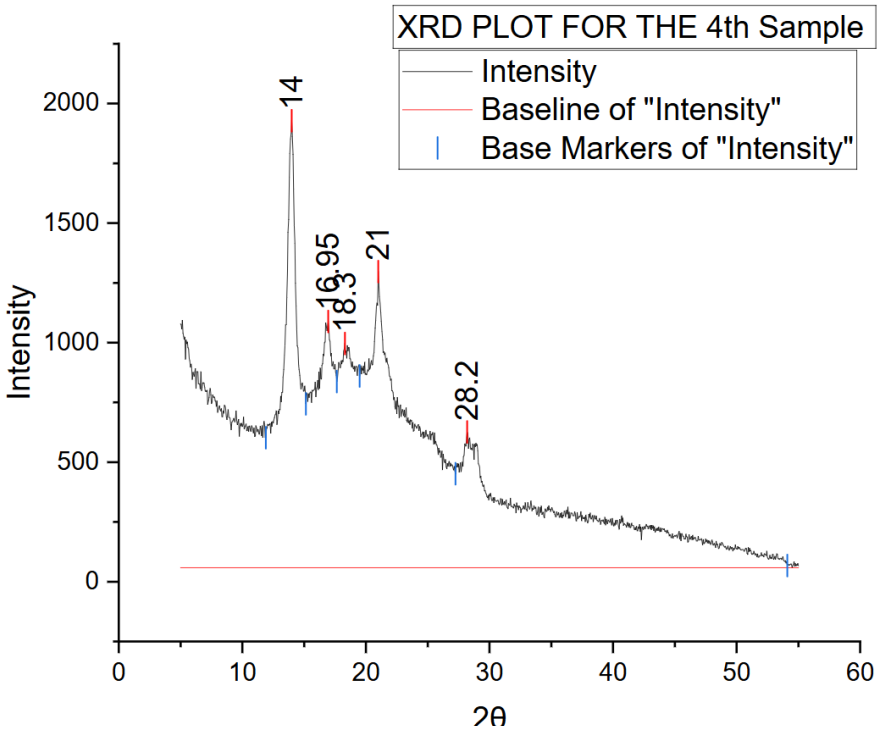

Figure II.10: pattern for the 4th Asphaltene Sample.

Figure (III.10) shows the pattern for the 4th sample. It also has a strong, sharp peak from waxy material with the same peak angle (2θ ≈ 14◦).

• **Distance between waxy chains (d paraffin):**

The peak is at 2θ ≈ 14.0◦, so θ ≈ 7.00◦.

7.00 × (π/180) ≈ 0.1222 radians

$$dparaffin = \frac{\lambda}{2\,sin(\theta)} = \frac{1.5406\,\text{Å}}{2\,sin(0.1222\ ^\circ)} \approx 6.32\text{Å} \qquad \text{II-9}$$

• **Distance for other side chains (dr = dγ)**: The peak is at 2θ ≈ 16.95 ◦, so θ ≈ 8.475◦

8.475 × (π/180) ≈ 0.1479 radians

$$\mathbf{d\gamma} = \frac{\lambda}{2\sin(\theta)} = \frac{1.5406\text{Å}}{2\sin(0.1479\ ^\circ)} \approx 5.23\text{Å} \qquad \text{II-10}$$

• **Distance between aromatic sheets (dm = d002):** The peak is at 2θ ≈ 21.00◦, so θ ≈ 10.50

10.50 × (π/180) ≈ 0.1833 radians

$$\mathbf{d002} = \frac{\lambda}{2\sin(\theta)} = \frac{1.5406\text{Å}}{2\sin(0.1833\ ^\circ)} \approx 4.24\text{Å} \qquad \text{II-11}$$

• **Average width of aromatic sheets (La):**

Initial conversion of FWHM and 2θ values from degrees to radians is required:

• ω10 (FWHM in radians) = 3.798° ×(π/180) ≈ 0.0663 radians

• θ10 (half of 2θ in radians) = (21.00/2) × (π/180) = 10.50 × (π/180) ≈ 0.1833 radians

$$La = \frac{1.84\lambda}{\omega \cos\theta_{10}} \approx 43.50\ \text{Å} \qquad \text{II-12}$$

• **Average height of aromatic stack (Lc):**

Utilizing the same FWHM and 2θ values (in radians) as for La

$$Lc = \frac{0.9\lambda}{\omega \cos\theta_{002}} \approx 21.28\ \text{Å} \qquad \text{II-13}$$

• **Average number of sheets per stack (M):**

$$M = \frac{L_C}{d_{002}} = \frac{21.28A^0}{4.24A^0} \approx 5.02\ \text{sheets} \qquad \text{II-14}$$

•**Number of Aromatic Rings (Ra):** Ra is estimated using the calculated La value:

$$R_a = \frac{La}{3{,}35A^o} - 1 = \frac{43.50A^o}{3{,}35A^o} - 1 = 12.985 - 1 \approx 11.98 \qquad \text{II-15}$$

Peak Numbers	FWHM	Center(2theta)	Height
1	2.249	14	1606.5
2	2.55	16.8	1159.87
3	2.5	18.45	1182.95
4	5.88	21.15	1373.24
5	2.22	28.85	758.28

Table II.1:Peak Data for the 3th Sample (From Origin)

Peak Number	FWHM	Center(2theta)	Height
1	0.991	14	1869.37
2	2.45	16.95	1029.74
3	1.8	18.3	937.48
4	3.798	21	1238.64
5	2.699	28.2	567.8

Table II.2: Peak Data for the 4rd Sample (From Origin).

II.7.3. Summary of Calculated Structural Parameters

Table (III.3) provides the outcome of full calculations for structural parameters of both asphaltene samples, from FWHM and Center (2θ) values, with an X-ray wave length of λ = 1.5406 ˚A.

Parameter	3rd Sample	4th Sample
Lc (°A)	13.74	21.28
La (°A)	28.1	43.5
Ra (Numbers of Rings)	7.39	11.98
d002 (°A)	4.2	4.24
dγ (°A)	4.81	5.23

M(Sheets/Stack)	3.27	5.02

Table II.3: Key Structural Parameters for Asphaltene Samples.

II.8. Results Interpretation:

XRD experiment on the Hassi Messaoud field asphaltene sample has provided very good information on their molecular structure and organization

II.8.1. Presence of Paraffinic Components

There is a clear, sharp peak of approximately 2θ = 14.0 degrees (peaks numbers Tables (III.1) and (III.2)) of the two samples are characteristic of waxy crystalline materials, that is long-chain paraffins. The presence of this particular peak is evidence that the asphaltene samples contain a large proportion of these ordered aliphatic units. This is of significant relevance, as Heavy paraffins can co-precipitate with asphaltenes, contributing in deposition issues in crude oil production and transport. This leads us to the conclusion that the waxy fractions cannot be totally soluble in common solvents, and thus be accountable for their unique diffraction signature.

II.8.2. Dimensions of aromatic core (Lc, La, Ra):

The computed values of Lc, La, and Ra provide a deep insight into the aromatic core architecture

II.8.2.1. Lc (Crystallite height):

The sample number 4 has much larger Lc (21.28
compared with the 3rd sample (13.74 ˚A). This suggests that the aromatic cores in the 4th sample are composed of a larger number of stacked aromatic layers.

II.8.2.2. La (Crystallite Diameter):

As with the Lc values, sample 4 (La = 43.50 ˚A) compared to sample 3 (La = 28.10 ˚A), has significantly larger aromatic sheets, meaning that there is a more prominent aromatic core in sample 4, probably due to larger aromatic sheet.

II.8.2.3. Ra (Number of Aromatic Rings):

The calculated Ra values also support these observations measurements. The sample number 4 has about an Ra of 11.98, while the sample number 3 has Ra of 7.39. This difference

illustrates the more sophisticated and richer character of the aromatic core of the 4th one's sample with more extensive aromatic ring condensation.

II.8.3. Inter-sheet Spacing (d002):

The d002 values, indicative of the interlayer spacings of piled aromatic sheets, we are typically observed in the range of values between 4.20-4.24 ˚A. They indicate such that aromatic sheets do not overlap one upon another. Loose packing is generally caused steric hindrance resulting from bulky aliphatic side groups attached to the aromatic backbone, which functioning as spacers hindering further piling up. These results validate past explanations with respect to the impact of waxy side chains on the aromatic lamellae's stacking structure.

II.8.4. Asphaltene Heterogeneity:

There exist definite differences observed in Lc, La, and Ra values of the 3rd and 4th samples highlight the intrinsic heterogeneities of asphaltenes. Even within samples from the same geographical area, molecular structural differences can be detected. This means asphaltenes consist of not one particular molecular species but of an intricate mixture of diverse molecular species together, ultimately bringing about the resulting structural elements. In addition, we can conclude that the island and archipelago structures may be present in the asphaltene of Hassi Messaoud.

II.9. Conclusion:

This X-ray Diffraction (XRD) analysis of the Hassi Messaoud field asphaltene samples has been informative of their structural features. The common premise for both sample sets is their large amount of paraffinic crystalline matter, as indicated from the sharp diffraction peaks. Wax content would be expected to influence the rheological properties and deposition tendency of these asphaltenes. Aside from this, the computed structural parameters (Lc, La, and Ra) have identified particular features of the aromatic cores of the asphaltenes. The 4th sample, for example, has larger and more compact aromatic layers with more fused rings and more height of stacks, compared with the 3rd sample. The structural differences, even for the same origin of the sample sets, are proof of the intrinsic complexity and heterogeneity of asphaltenes.

Finally, the relatively large values of d002 indicate less compact stacks of aromatic sheets, caused largely through steric hindrance from bulky aliphatic side chains. Such general characterization of such intricate structural entities is most essential for accurate predictions of asphaltenes' behavior, particularly deposition tendency. This will be helpful towards more effective strategies for mitigating asphaltene-related issues during production of crude from the Hassi Messaoud field.

Chapter III: Crude oil Evaluation and Flow Assurance of OMM-33.

III.1. Introduction

Effective management of the asphaltene deposition challenges necessitates a thorough understanding of the crude oil's properties and its asphaltene behavior under various production scenarios. This chapter presents a detailed case study focusing on the flow assurance characteristics of representative crude oil samples from the OMM-33 well in Hassi Messaoud field, primarily based on data presented in the Schlumberger Reservoir Laboratories report. The study encompasses a Pressure-Volume-Temperature (PVT) analysis, determination of Asphaltene Onset Pressure (AOP) under different thermal conditions, and an experimental evaluation of asphaltene deposition tendency using a dynamic flow loop. The objective of this study is to obtain essential data that can help in reservoir engineering analysis, simulation and surface facilities design.

III.2. Fluid Characterization and PVT Analysis of OMM-33 Crude:

Understanding the reservoir fluid properties is the first step in any flow assurance study. This section details the characterization of the Hassi Messaoud crude oil samples from well OMM-33. We get ten samples at deferent depth**,** the samples are:

Sample ID	**Cylinder ID**	**Opening Conditions in the Lab**	**Field Reported Sample Volume**
		psia at °C	**cm^3**
1.01	9271-MA	5147 at 24.6	520
1.02	22300-IB	5119 at 24.6	520
1.03	22405-IB	5200 at 24.6	520
1.04	8245-MA	5488 at 24.6	520
1.05	21857-IB	5742 at 24.6	520
1.06	22329-IB	5030 at 23.7	520
1.07	21849-IB	5720 at 24.8	500

1.08	21860-IB	5743 at 24.8	500
1.09	21453-IB	5100 at 23.7	520
1.10	22335-IB	5377 at 24.8	500

Table III.1: Initial Sample Validation Results. [28]

III.2.1. Crude Oil Composition:

A detailed compositional analysis extending to C36+ was performed using gas chromatography (GC) on ten individual bottomhole samples. The averaged molar composition of the reservoir fluid, derived from these ten samples, is presented in **Table (III.3)**

Component	MW (g/mol)	Average Reservoir Fluid (mole %)
CO2	44.01	1.738
H2S	34.08	0
N2	28.01	1.883
C1	16.04	24.044
C2	30.07	11.879
C3	44.1	10.363
i-C4	58.12	1.428
n-C4	58.12	5.432
i-C5	72.15	1.541
n-C5	72.15	2.95
C6	84	3.694
Mcyclo-C5	84.16	0.543
Benzene	78.11	0.346
Cyclo-C6	84.16	0.433
C7	100.21	3.248
Mcyclo-C6	98.19	0.86
Toluene	92.14	0.32
C8	114.23	3.356
C2-Benzene	106.17	0.204
m&p-Xylene	106.17	0.42
o-Xylene	106.17	0.17
C9	128.26	2.679
C10	134	3.257
C11	147	2.523
C12	161	2.117
C13	175	1.921
C14	190	1.532
C15	206	1.391

C16	222	1.14
C17	237	0.967
C18	251	0.874
C19	263	0.788
C20	275	0.664
C21	291	0.593
C22	305	0.518
C23	318	0.452
C24	331	0.397
C25	345	0.358
C36+	583.63	0.861
Total	—	99.998

Table III.2: Averaged molar composition for Hassi Messaoud (OMM-33) reservoir fluid, derived from ten bottomhole samples. [28]

III.2.2. PVT Analysis and Phase envelope Modeling:

The PVT behavior of the HMD crude was modeled using an Equation of State (EoS), tuned with experimental data from the OMM-33 samples. Key average parameters for the samples include a reservoir temperature of 122◦C and initial reservoir pressure around 2858psia (197bar). The predicted saturation (bubble point) pressures at various temperatures, averaged from the ten samples, are crucial for understanding the fluid's phase envelope (Table III.3). conceptually illustrates a typical phase envelope derived from such data.

Temperature (°C)	Average Bubble Point Pressure (bar)
120	123.6
90	110.9
75	103.7
56	94.1

Table III.3: Average predicted bubble point pressures for Hassi Messaoud (OMM-33) crude oil samples at various temperatures. [28]

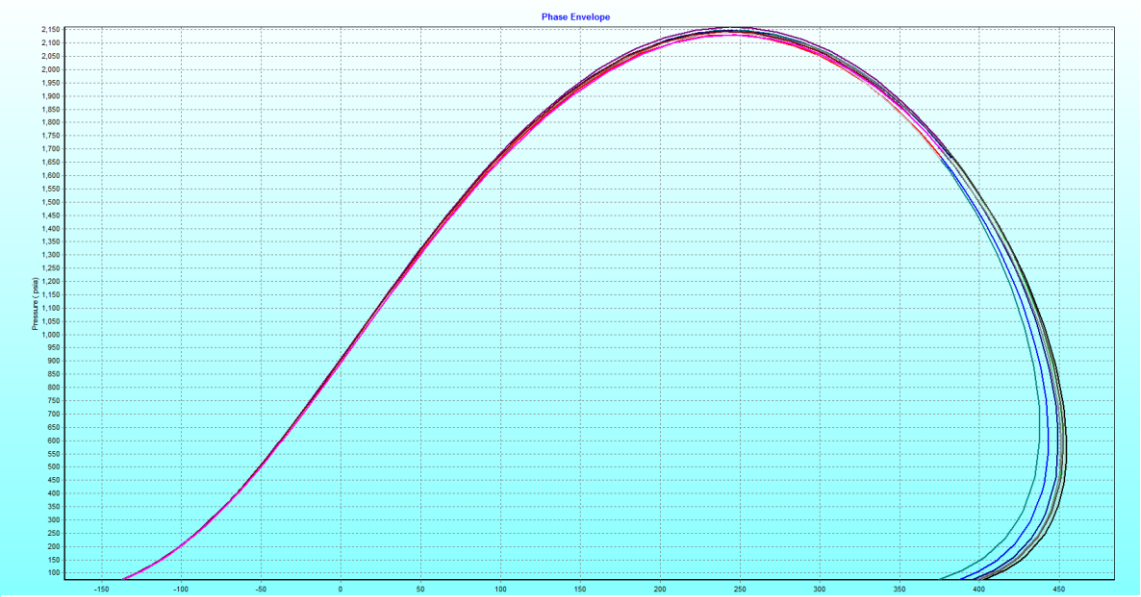

Figure III.2: Conceptual simulated phase envelope for OMM33 for the ten samples crude oil. [28]

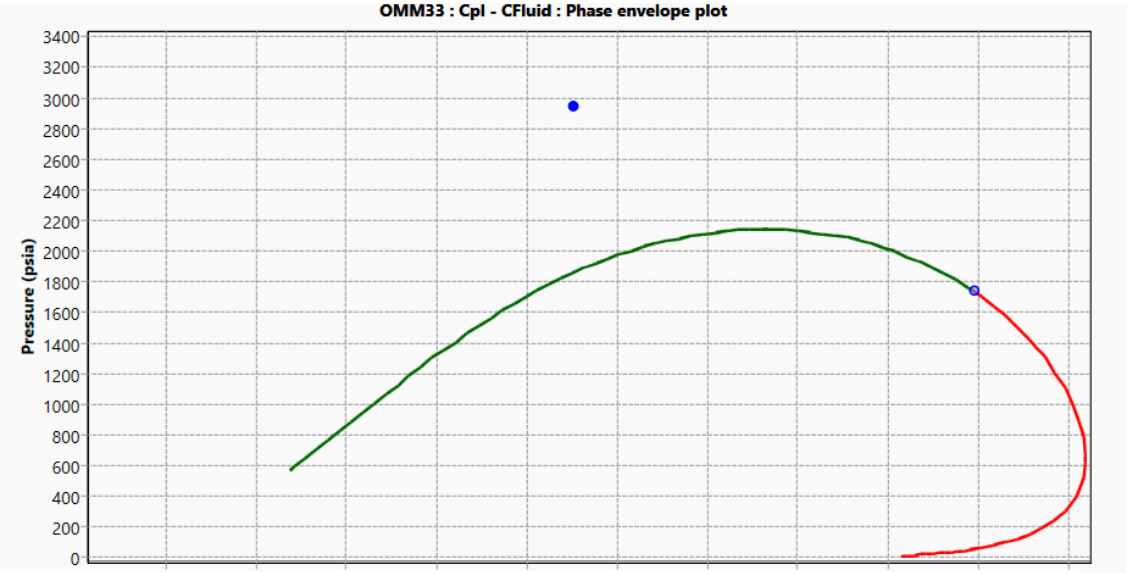

Figure III.1: 2Conceptual simulated phase envelope for OMM33 for average fluid composition.

III.3. Asphaltene Content Measurement:

Prior to the asphaltene content measurements, sample 1.01, 1.02, 1.03, 1.07, 1.08 and 1.09 were conditioned at reservoir temperature and 10000psig for 5 days to ensure sample homogeneity prior to testing. To assure consistency, samples 1.02, 1.03 and 1.08 were

transferred into a 2-liter recombined cylinder, CSB 16226-EB. Also, samples 1.01, 1.06, 1.09 were transferred into a 2-liter recombined cylinder, CSB 14460-EB.

A heated isobaric push off was performed to collect sub-samples from each CSB 16226-EB and CSB 14460-EB for asphaltene content measurement.

The asphaltene content measurement were performed on both whole oil (as collected from cylinders) and on the topped oils after removal of light ends. The results are presented in table (III.4).

Sample ID	Asphaltenes (wt %)Whole Oil	Asphaltenes (wt %)Topped Oil
1.02+1.03+1.08	0.30	1.83
1.01+1.06+1.09	0.31	1.96

Table III.4: Asphaltene Content Measurement. [28]

III.4. Asphaltene Onset Pressure (AOP) for OMM-33 Crude oil:

The AOP defines the boundary of asphaltene stability. Excursions below this pressure can trigger precipitation.

III.4.1. Experimental Determination of AOP:

The Asphaltene Onset Pressure (AOP) for the HMD crude oil (sample 1.10, SSB 22335-IB, from well OMM-33) was experimentally determined using an isothermal depressurization technique. This method measures the pressure at which asphaltenes begin to precipitate from the live oil under constant temperature conditions.

III.4.1.1. Methodology and Apparatus:

- **Sample Conditioning:** Prior to testing, the live oil sample was restored to ensure it was a single-phase, homogenous fluid. It was conditioned at reservoir temperature (122°C) and a pressure of 10,000 psig, well above the expected AOP and reservoir pressure, for five days with continuous agitation. This process re-dissolves any asphaltene particles that may have precipitated during sampling and transport.

- **Apparatus:** The analysis was conducted using a high-pressure, temperature-controlled visual PVT cell, referred to as the Organic Solid System (OSS). This system is equipped with a high-precision solids detection system (SDS) utilizing fiber optic probes. These probes transmit a Near-Infrared (NIR) laser beam through the fluid to monitor its optical transmittance.

- **Measurement Principle:** The AOP is identified by a distinct change in the NIR light transmittance. As the fluid is depressurized, its density decreases, which typically causes a gradual increase in light transmittance. The onset of asphaltene precipitation, however, leads to the formation of solid particles that scatter and absorb the light, causing a sharp and sustained drop in the measured transmittance. This inflection point defines the AOP.

III.4.1.2. Isothermal Depressurization Procedure:

The conditioned sample was isobarically and isothermally charged into the OSS cell. A series of tests were performed at three different temperatures to map the asphaltene precipitation envelope.

- **Test 1 (90°C):** The cell was maintained at a constant temperature of **90°C**. The pressure was then gradually reduced from **10,000 psig down to 1,700 psig** at a controlled rate of **100 psi/min**. The bubble point pressure at this temperature was noted to be approximately 1,760 psia.

- **Test 2 (75°C):** The procedure was repeated at a constant temperature of **75°C**. The pressure was reduced from **10,000 psig to 2,086 psig**.

- **Test 3 (56°C):** A final test was conducted at a constant temperature of **56°C**, with pressure reduced from **10,000 psig to 1,000 psig**.

III.4.2. AOP Results and Discussion:

The AOP measurements for the HMD crude (sample 22335-IB) at temperatures of 90◦C, 75◦C, and 56◦C are summarized in Table (IV.5). Representative NIR transmittance curves are conceptually shown in figure (III.3,4,5).

Temperature (°C)	Asphaltene Onset Pressure (psig)
90	4120
75	3690
56	3180

Table III.5: Asphaltene Onset Pressure (AOP) measurements for Hassi Messaoud (OMM 33, sample 22335-IB) crude oil using NIR technique. [28]

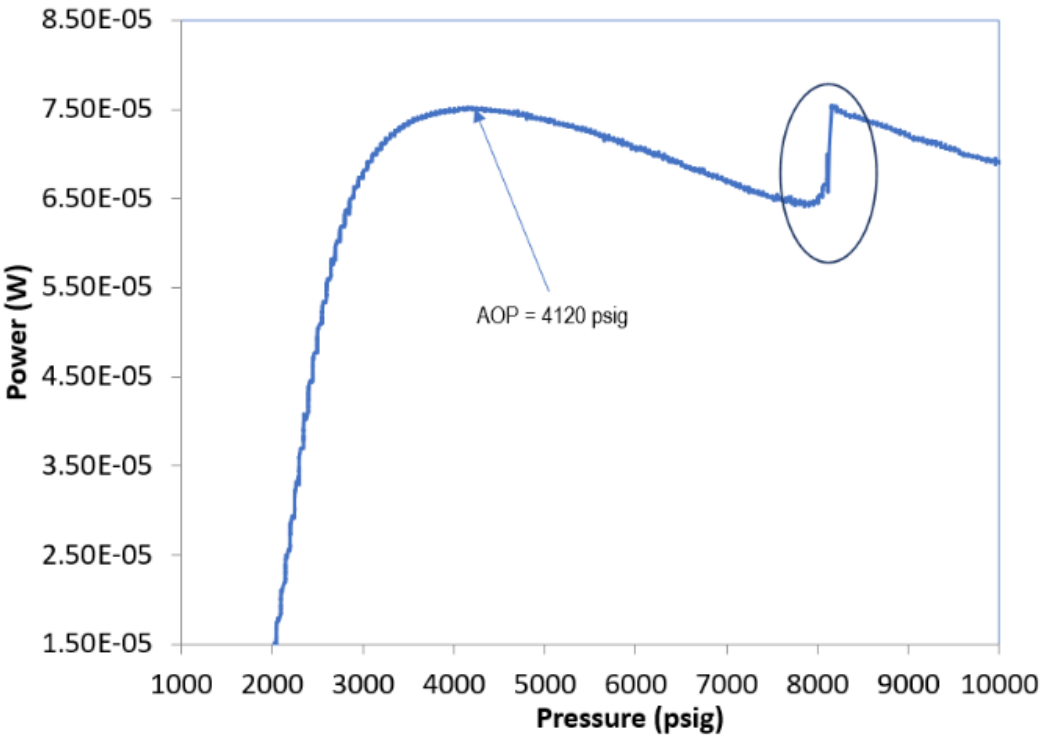

Figure III.3: (a) AOP at 90◦C [28]

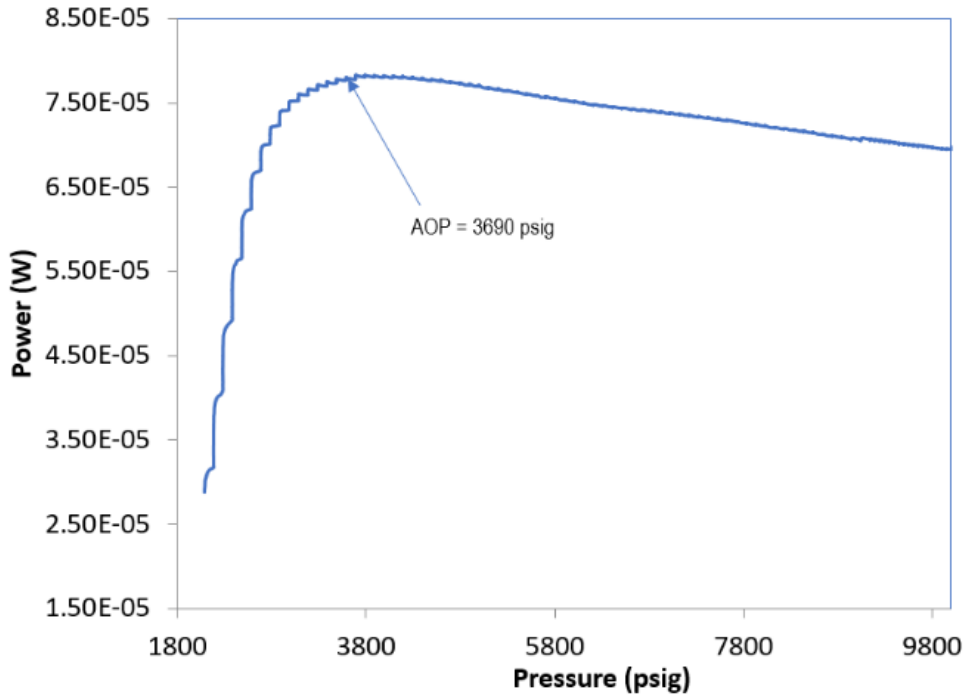

Figure III.4: (b) AOP at 75◦C [28]

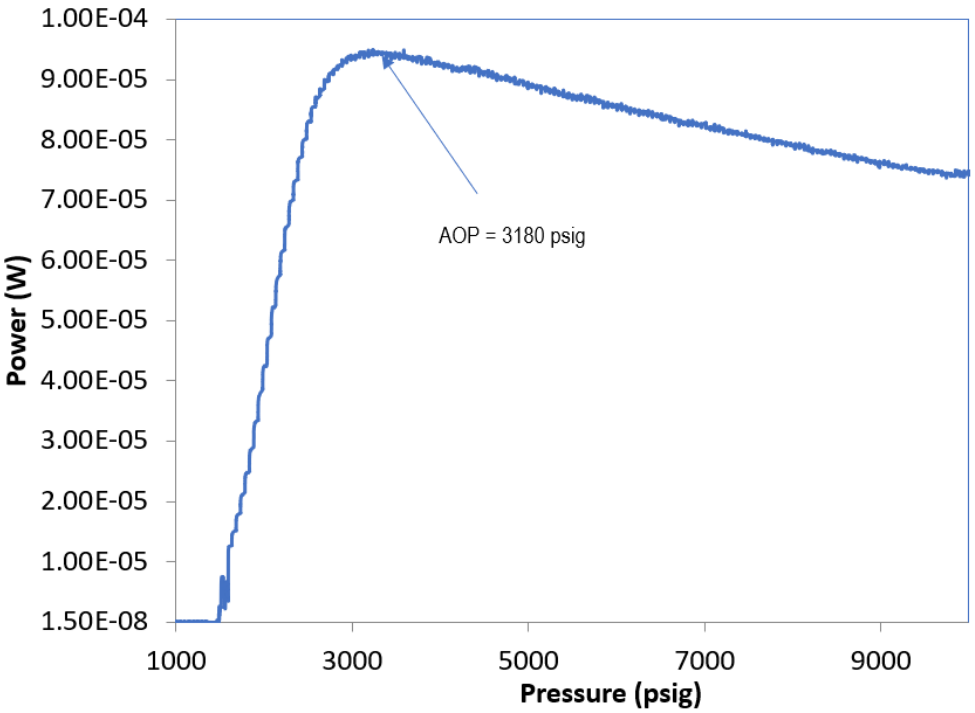

Figure III.5: (c) AOP at 56◦C [28]

Using all the previews Data (Composition, AOP) we can make PVT envelope (Figure III.6) and a risk curve similar to as represented in the figure bellow which represents many well in zone 01 and 23 and the curve for asphaltene precipitation:

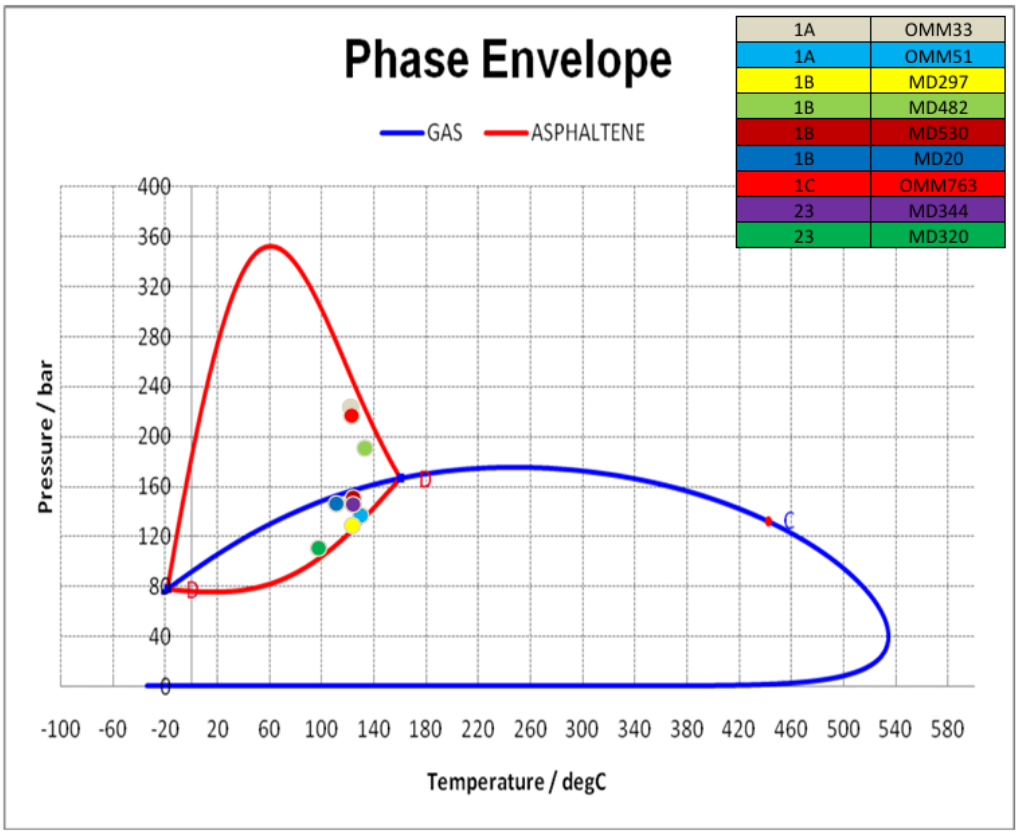

Figure III.6: risk curve for asphaltene precipitation. [1]

Figure III.3,4,5: Conceptual Near-Infrared (NIR) responses during isothermal depressurization tests for AOP determination of Hassi Messaoud crude OMM33 (sample 22335-IB). (a) (b) (c)

For instance, at 90◦C, the AOP is 4120psig, while the average bubble point is 110.9bar (≈ 1608psig). This implies that asphaltene precipitation can occur in the single-phase liquid region well before gas liberation. The AOP decreased with decreasing temperature within the range tested. The AOP values are significantly higher than the initial reservoir pressure (around 2858psia), which, as discussed in the source report of Schlumberger , might suggest that asphaltenes were out of solution at the sampling point or that repressurization during sample restoration redissolved precipitated asphaltenes, leading to an apparently higher lab-measured AOP.

III.5. Experimental Asphaltene Deposition Study (Flow Assurance Test):

Dynamic deposition tests quantify asphaltene deposition under flowing conditions**.**

III.5.1. Deposition Test Methodology:

Asphaltene deposition tendency for blended HMD crude samples was evaluated using the **RealView** deposition cell, simulating pipeline flow conditions. Live crude oil was flowed through the test cell under controlled conditions of temperature, pressure, and shear rate, simulating field production parameters Tests were conducted at 90◦C (sample blend CSB 16226-EB) and 75◦C (sample blend CSB 14460-EB) with system pressures of **1950 psig** and **1850 psig** respectively, slightly above their bubble points but likely below their AOPs. Approximately **1825 cc** of live oil was flowed through the cell. Deposited material was recovered by DCM washing and quantified.

Pipeline Information	
Production rate (bbl/day)	581.196
Pipe ID (in)	3.92
Average velocity (m/s)	0.137365
Reynolds number	22089
Friction factor	0.0063
Wall shear stress (Pa)	0.0385
Wall shear rate (1/s)	96.2

Table III.6:Field Conditions used for the RealView Testing. [28]

Production Rate	**Pipe Type**	**Spindle Speed**
m3.hr	-	Hz
3.85	4.5” NV 13.5#	10

Table III.7:Field Production Conditions, RV Spindle speed. [28]

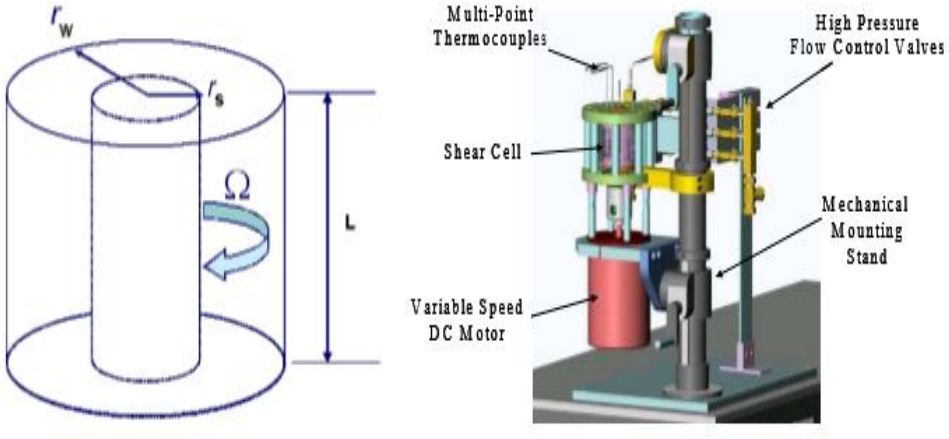

Figure III.7: The RealView Apparatus Based on the Taylor-Couette Principle [28]

III.5.2. Deposition Results and Characterization:

The mass of asphaltene deposited on the cell wall and end caps is presented in Table (II.8). Visual inspection of the cell components post-test provided qualitative information on the deposit morphology **(Figure III.7).**

Test Temperature (°C)	Sample ID	Wall Deposit Mass (mg)	End Caps Mass (mg)
90	CSB 16226-EB	52.3	28
75	CSB 14460-EB	25.3	44.2

Table III.8: Summary of asphaltene deposit mass from RealView deposition tests on Hassi Messaoud (OMM-33) blended crude samples. [28]

RealView wall, End caps and Spindle images prior to Rinse:

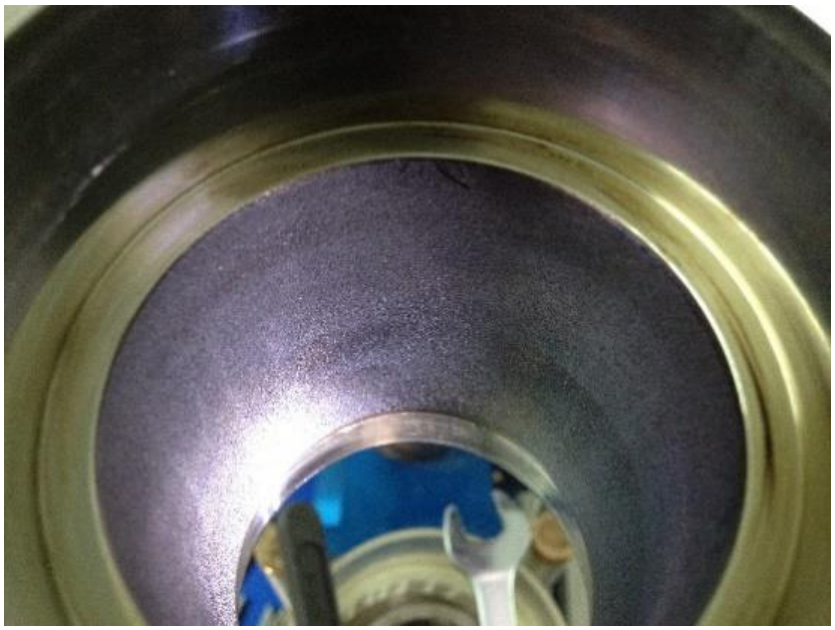

Figure III.8:Wall-Deposition Test 90°C-Run 1[28]

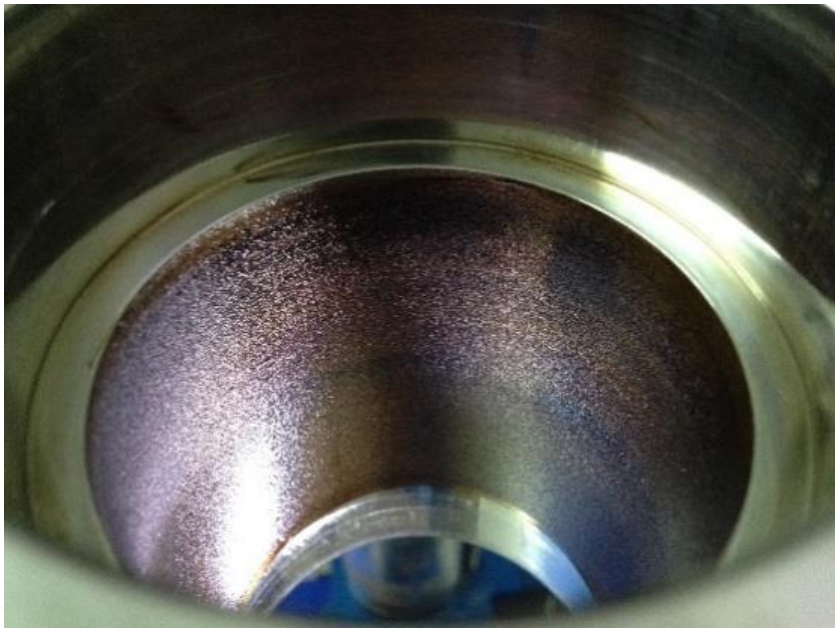

Figure III.9: Wall- Deposition Test 75°C-Run 2[28]

Figure III.10: Bottom and TopEnd Caps and Spindle- Deposition Test 75°C- Run 2 [28]

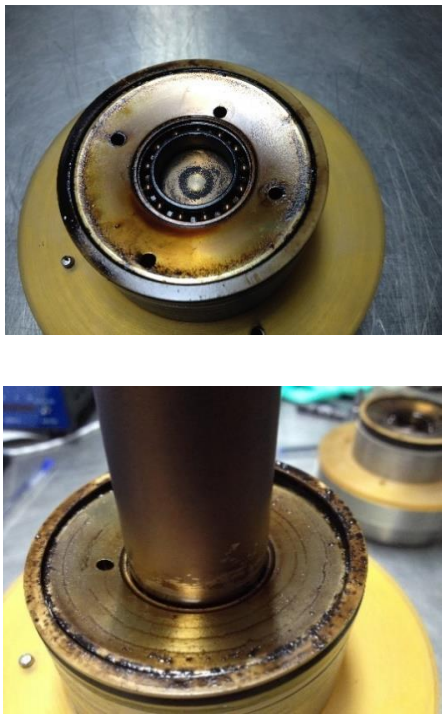

Figure III.11: Bottom and TopEnd Caps and Spindle- Deposition Test 90°C- Run 1 [28]

The SARA analysis of the true deposits (Table III.8) revealed a very high asphaltene content for the deposit formed at 90◦C (97.7 wt% asphaltene on the wall). The deposit at 75◦C

surprisingly showed a lower asphaltene content (44.4 wt% on the wall), suggesting co-precipitation or a different deposit nature at this lower temperature, which warrants further investigation**.** [28]

Test Temp. (°C)	Sample ID	Deposit Location	Asphaltene (wt%)	Other (wt%)
90	CSB 16226-EB	Wall	97.7	2.3
		End Caps	97.5	2.5
75	CSB 14460-EB	Wall	44.4	55.6
		End Caps	57.6	42.4

Table III.9: SARA analysis of asphaltene deposits from RealView tests on Hassi Messaoud (OMM-33) blended samples. [28]

♦ Conclusion:

This thesis presents a focused investigation into the proprieties of asphaltenes in the Hassi Messaoud field, with special emphasis on advanced analytical methods and flow assurance considerations. The study centered on four core areas: **X-ray Diffraction (XRD)** analysis, **Pressure-Volume-Temperature (PVT)** characterization, **Asphaltene Onset Pressure (AOP)** determination, and **experimental deposition testing**.

The **XRD analysis** of Hassi Messaoud asphaltenes revealed significant paraffinic crystallinity in combination with loosely stacked aromatic layers. The measured interlayer distances (d002 ≈ 4.2 Å) and lateral sizes of aromatic cores confirmed the structural heterogeneity of asphaltenes—an important factor in their unpredictable precipitation behavior.

Through **PVT studies**, crude oil samples from well OMM-33 were characterized using real bottomhole data. The fluid exhibited complex phase behavior, and the modeling of its thermodynamic properties allowed for accurate simulation of conditions leading to asphaltene instability.

Most critically, the **Asphaltene Onset Pressure (AOP)** values were found to exceed both the bubble point and the initial reservoir pressure—implying that asphaltene precipitation may initiate even while the fluid remains in the single-phase liquid region. This behavior poses a major threat to flow assurance and production sustainability.

Deposition tests carried out under dynamic conditions further demonstrated the high risk of solid accumulation. Results confirmed that temperature significantly influences the nature of deposits—ranging from heavy asphaltene-rich layers at higher temperatures (e.g., 90°C) to mixed organic residues at lower temperatures (e.g., 75°C).

In conclusion, the integration of **XRD structural analysis, thermodynamic modeling, AOP detection, and flow loop experiments** provides a clear understanding of the asphaltene behavior in Hassi Messaoud. The findings highlight the necessity of developing advanced, tailored mitigation strategies to overcome the limitations of conventional treatments and ensure reliable flow assurance in asphaltene-prone reservoir.

Research Horizons for Future Work:

- Extend characterization to other zones within Hassi Messaoud to determine variation in asphaltene behavior across the reservoir.
- Use NMR or FTIR for more detailed structural into heteroatoms and chemical bonds and functional groups.
- Introducing TGA (thermogravimetric analysis) to evaluate the thermal stability of asphalt and predict contamination under thermal enhanced oil recovery processes.
- investigate nanoparticle-enhanced inhibition or smart chemical inhibitors to prevent precipitation and deposition in field pipelines or wellbores.
- Study the use of ultrasonic and microwave technologies for changing asphaltene behavior, rheology, and crude oil viscosity.

Reference:

1. M. C. Henni, Formation Damage Prevention Through Organic Deposit Control in Hassi Messaoud Oil Field, M.S. thesis, Dept. Oil and Gas Production Eng., 2011.
2. Nouacer, A. Collaku, and I. Bendjedia, "Challenges for digital oil field applications in Hassi-Messaoud Field (HMD), Sonatrach, Algeria," presented at the SLB SIS Forum, Schlumberger, Sept. 18, 2019.
3. Zeroug and N. Bounoua, Eds., "Chapter 1," in Well Evaluation Conference – Algérie 2007, Sonatrach & Schlumberger, p. 3, 2007.
4. A. M. Zerdazi, R. Belhadi, and N. Bouhadi, "Structural control and petroleum potential of the Hassi Messaoud field, Algeria," Journal of Petroleum Geology, vol. 33, no. 3, pp. 233–250, 2010.
5. A. S. Bouzidi, M. Kaced, and H. Guermessa, "Lithostratigraphic and Petrophysical Analysis of Cambrian Sandstone Reservoirs in Hassi Messaoud Field, Algeria," Journal of African Earth Sciences, vol. 112, pp. 190–202, 2015.
6. Touil, "Caractérisation physico-chimique des asphaltènes d'un brut algérien: Cas du champ de Hassi Messaoud," Master's thesis, Université Kasdi Merbah Ouargla, 2022. [Online]. Available: https://dspace.univouargla.dz/jspui/bitstream/123456789/37151/1/Touil%20Adem.pdf
7. Sonatrach, Hassi Messaoud Reservoir Characterization and Zoning Report, Internal Technical Report, Algiers, Algeria, 2010.
8. H. Ait Ouarab, "Sedimentology and diagenesis of the Cambro-Ordovician reservoir rocks of the Hassi Messaoud field (Algeria)," Doctoral dissertation, University of Hamburg, 2003. https://ediss.sub.uni-hamburg.de/bitstream/ediss/778/1/PhD-Thesis.pdf
9. R. F. Meyer, J. W. Schmoker, and L. W. Law, "Geologic assessment and production performance of large oil fields," AAPG Bulletin, vol. 85, no. 9, pp. 1569–1601, 2001.
10. M. Tavakkoli and F. M. Vargas, "Chapter 1: Introduction to asphaltene deposition," in Asphaltene Deposition Fundamentals, CRC Press, 2016, pp. 1–20.
11. J. H. Gary, G. E. Handwerk, and M. J. Kaiser, Petroleum Refining: Technology and Economics, 5th ed., Boca Raton, FL, USA: CRC Press, 2007.

12. J. G. Speight, The Chemistry and Technology of Petroleum, CRC Press, 2006, ch. 2.
13. Kimray, "Oil & Gas 101: Introduction to oil and gas production." [Online]. Available: https://kimray.com/learning/oil-gas-101
14. M. Hassanzadeh and J. Abedi, "Asphaltene deposition in production tubing in an oilfield in the Gulf of Mexico," ResearchGate. [Online]. Available: https://www.researchgate.net/figure/Asphaltene-deposition-in-production-tubing-in-an-oilfield-in-the-Gulf-of-Mexico_fig2_351735385
15. World Iron & Steel, "Why do you need remove the paraffin in oil pipelines?" Worldironsteel.com, June 10, 2021. [Online]. Available: https://www.worldironsteel.com/news/why-do-you-need-remove-the-paraffin-in-oil-pip-48079530.html
16. G. A. Mansoori, "Phase behavior in petroleum fluids (A Detailed Descriptive and Illustrative Account)," arXiv preprint, arXiv:1711.04200, 2017.
17. WaterWorld, "Scale factors: Reducing corrosion in pipelines with electronic water treatment." [Online]. Available: https://www.waterworld.com/home/article/16192780/scale-factors-reducing-corrosion-in-pipelines-with-electronic-water-treatment
18. Nfatmala, "Hydrate/Wax/Asphalt in subsea pipeline," Blogspot, Feb. 2016. [Online]. Available: https://nfatmala.blogspot.com/2016/02/hydratewaxasphalt-in-subsea-pipeline.html
19. M. Ashraf-Khorassani, L. T. Taylor, R. P. Rodgers, A. G. Marshall, and S. R. Larter, "Structural characterization of asphaltenes: Comparison of mass spectrometric and spectroscopic methods," The Analyst, vol. 141, no. 1, pp. 306–315, 2016.
20. T. F. Yen and G. V. Chilingarian, Asphaltenes and Asphalts, 1: Developments in Petroleum Science, vol. 40A, Amsterdam, The Netherlands: Elsevier, 1994.
21. Alamy, "Fourier Transform Infrared Spectroscopy (FTIR) spectrometer in forensics lab," [Photograph]. [Online]. Available: https://www.alamy.com/stock-photo-fourier-transform-infrared-spectroscopy-ftir-spectrometer-in-forensics-29362233.html
22. O. C. Mullins, "The modified Yen model," Energy & Fuels, vol. 24, no. 4, pp. 2179–2207, 2010.
23. Encyclopaedia Britannica, "Bragg law." [Online]. Available: https://www.britannica.com/science/Bragg-law

24. R. M. Vázquez, “Components of a diffractometer,” ResearchGate, 2020. [Online]. Available:
https://www.researchgate.net/figure/Components-of-d iffractometer_fig2_355201732
25. R. J. Miranda, G. R. Furlan, M. B. Saldanha, J. C. C. Freitas, and A. G. Lago, “The origin and nature of asphaltenes: Revisiting fundamental aspects,” Journal of Molecular Biology, vol. 433, no. 24, p. 167278, 2021.
26. D. P. Miller and P. York, “Powder X-ray patterns of (a) amorphous and (b) crystalline sucrose,” in Crystalline and Amorphous Forms of Pharmaceuticals, ResearchGate, 2004. [Online]. Available: https://www.researchgate.net/figure/Powder-X-ray-patterns-of-a-amorphous-and-b-crystalline-sucrose_fig7_7629281
27. A. Benaouicha, N. A. Bouteraa, and M. Belbachir, “Influence of asphaltene on the physicochemical properties of Algerian Hassi Messaoud crude oil,” React. Kinet. Mech. Catal., vol. 140, pp. 365–378, 2023, https://link.springer.com/article/10.1007/s11144-023-02514-9
28. Schlumberger Reservoir Laboratories, “Fluid analysis final report: Black oil sample validation and flow assurance study (Well OMM-33, Hassi Messaoud),” Internal Company Report No. 2016DZH1-P021-J0067, prepared for Sonatrach-DP-HMD, May 17, 2018.